ORIGINAL ARTICLE

Green approach on pretreatment of rice straw using deep eutectic solvent for lignin recovery and efficient hydrolysis

Shiva Lall Sunar[1] · Debraj Bhattacharyya[2,3] · Gayathri Vanniappan[3] · Tarun K. Panda[1]

Abstract

The use of green processes to recover valuable products from lignocellulosic biomass has gained attention in recent years. In this work, rice straw biomass was pretreated using a natural deep eutectic solvent (NADES), composed of naturally occurring reagents, namely, choline chloride (ChCl) and L-(+)-tartaric acid (TA). The NADES-ChCl/TA was investigated as a potential solvent for the fractionation of rice straw into cellulose-enriched material (CEM) with simultaneous lignin recovery. During the process development, the variables considered were temperature, time, and DES concentration with the experimental range of 96–140 °C, 100–180 min, and 14–40 v/v%, respectively. The experimental design facilitates the mixing of NADES-ChCl/TA with water, resulting in a lower viscosity of NADES which enables effective contact of NADES with rice straw biomass. The qualitative assessment of lignin removal from rice straw was observed using ATR/FT-IR spectra and X-ray diffraction. The pretreated rice straw during enzymatic hydrolysis showed a 6.5 times higher fermentable sugar yield than the untreated sample. The NADES-ChCl/TA showed excellent recyclability up to 8 cycles. The designed process could be considered a viable alternative to conventional biorefinery processes.

Keywords Deep eutectic solvent · Enzymatic hydrolysis · Lignin recovery · Resource recovery · Response surface methodology · Rice straw

1 Introduction

The generation of fuel based on renewable resources like solar, hydro, and energy is necessary due to the depletion of the world's petroleum reserves and related environmental problems. Lignocellulosic biomass (LCB) has emerged as a promising renewable resource because of its widespread availability. LCB, such as energy crops, forest, and agricultural residues, could be used as potential alternatives to fossil fuels because of their higher abundance and near-zero carbon footprint [1, 2]. Rice straw, an LCB source, is abundantly available. The annual production of rice straw around the globe ranges between 650 and 975 million tonnes; a fraction of this is used as cattle feed, and the remaining is considered waste and burned in the field [3]. The burning of rice straw deteriorates the air quality, which has a severe impact on public health. There is a rising interest in using this agri-residual waste as a renewable material. The complex structure of LCB makes it resistant to chemical and biological transformations. The LCB molecular structure comprises three primary components: cellulose, hemicellulose, and lignin, all of which can be transformed into value-added products [4]. The LCB-derived product includes platform chemicals, ethanol, and biochemicals [5, 6].

The cellulose is highly crystalline, surrounded by the hemicellulose, and the lignin makes up the outer protective layer, preventing the polysaccharides from coming in contact with water and other chemicals [7]. Thus, the primary components of LCB are difficult to recover due to their inherent complex structure. As a result, there is a need for fractionating LCB without losing materials. Therefore,

✉ Debraj Bhattacharyya
debrajb@ce.iith.ac.in

✉ Tarun K. Panda
tpanda@chy.iith.ac.in

1 Department of Chemistry, Indian Institute of Technology Hyderabad, Kandi, Sangareddy, Telangana 502284, India

2 Department of Civil Engineering, Indian Institute of Technology Hyderabad, Kandi, Sangareddy, Telangana 502284, India

3 Centre for Interdisciplinary Programs, Indian Institute of Technology Hyderabad, Kandi, Sangareddy, Telangana 502284, India

pretreatment of LCB is required to improve the LCB fractionization to fermentable sugars and other value-added chemicals [8]. One of the primary challenges in LCB valorization is finding suitable solvents for pretreatment that are both environmentally friendly and economical. In recent years, solvents like ionic liquids (ILs) have attracted great interest and have been widely utilized for LCB pretreatment due to their exceptional capability over conventional acid, base, or organic solvent–based methods [9, 10]. Efforts have been made to find novel ILs that are more advantageous than conventional solvents, but the ILs can be expensive because of the cost associated with their synthesis, and they have poor biodegradability which limits their usage on a large scale [11, 12]. As an environmentally friendly replacement for ILs with comparable qualities, lower cost, and greater atom economy, the use of deep eutectic solvents (DESs) in LCB processing has increased in recent years [13, 14]. DES are made up of two distinct substances that act as hydrogen bond acceptors (HBA, quaternary ammonium salts, etc.,) and hydrogen bond donors (HBD, carboxylic acids, amide, polyols, etc.) [15, 16]. The hydrogen bonding between HBA and HBD induces charge delocalization, resulting in a lower melting point for the combined substance (i.e., DES) compared to either component in pure form [17]. The use of DES as a green solvent for LCB pretreatment is considered an eco-friendly process in biorefinery and recovery of value-added chemicals.

The pretreatment of LCB rice straw has been reported in the literature using different DES combinations. For instance, Hou et al. employed DESs made from choline chloride (ChCl)/urea (CU), ChCl/oxalic acid (CO), and malic acid/pyroline to pretreat rice straw biomass [18]. Xing et al. have synthesized two-component and three-component DESs with choline chloride as HBA and formic acid (FA), acetic acid (AA), glycerol (Gly), and urea (U) as HBD for rice straw pretreatment and reported a lignin removal ranging between 43.6 and 79.8% affording high accessibility of cellulose recovery and glucose yield (Fig. 1) [19]. Zulkefli

Fig. 1 Certain illustration of DES pretreatment of LCB
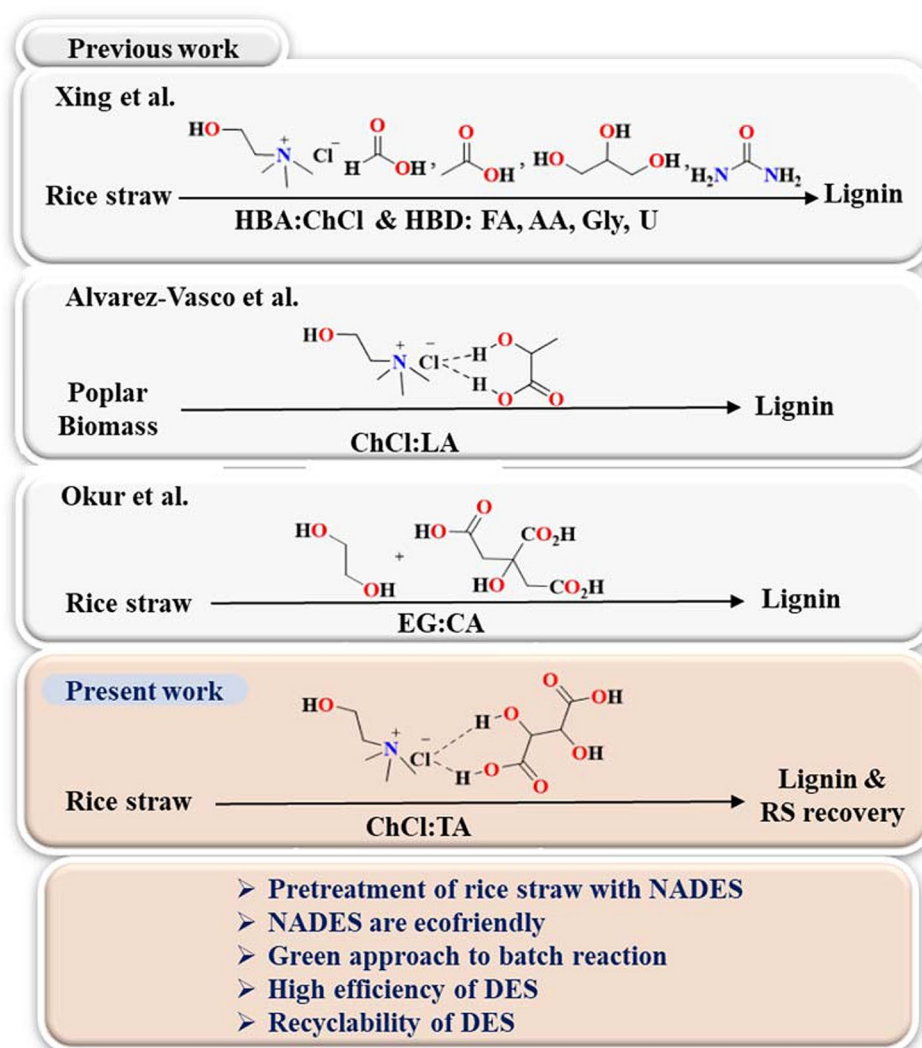
et al. employed ethylammonium chloride: ethylene glycol (EAC: EG) DES to treat oil palm trunk (OPT) and observed that 42% of the lignin and 83% of the hemicellulose had been removed [20]. Similarly, Okur and Eslek Koyuncu showed the effective delignification of rice straw using an ethylene glycol (EG)/citric acid (CA) DES system, where the maximum lignin removal of 57.33% was obtained at 120 °C for 4 h pretreatment [21]. Under relatively harsh conditions (145 °C, 6 h), Alvarez-Vasco et al. used a ChCl/lactic acid (LA) molar ratio of 1:2 to extract 78% of the lignin from poplar biomass [22]. These findings demonstrated the potential of DESs for biomass pretreatment. However, DES pretreatment of LCB is still in its early stage, and there are no systematic studies on LCB pretreatment with DES to enhance high lignin dissolution [23]. Thus, the pretreatment of LCB with DES requires further studies to develop new pretreatment methods. The solvents derived from natural systems such as carbohydrates are promising candidates for pretreatment since carbohydrates make up a major portion of LCB. The DESs synthesized using reagents from natural origin are termed natural deep eutectic solvents (NADESs) [24]. The reagents such as amino acids and sugars are available in the environment as natural compounds. Therefore, employing NADES pretreatment serves as a good way to utilize biomass more efficiently.

The most widely used NADESs were based on ChCl reagents (HBA) because of their facile synthesis, high purity, biodegradability, and lower chemical cost [25]. ChCl-based DES pretreatment approaches delignify the LCB by forming hydrogen bonds between -OH groups in lignin and halogen anions (Cl⁻) of deep eutectic solvent [26]. The quality of ChCl-based DES pretreatment could be tuned by adjusting HBD and their molar ratio with HBA. Also, the selection of HBDs could vary the chemical-physical properties of the DESs, affecting their performance [27–29]. For instance, acid HBDs offer an effective dissolution of LCB than that of basic and neutral HBDs [15, 25]. Furthermore, DES pretreatment depends on whether the HBD was monocarboxylic acid or dicarboxylic acid [30]. The high acidity and polarity of DES contribute to the lignin removal during LCB pretreatment [31]. Concerning DES acidity, TA (HBD) is diprotic and one of the strongest organic acids that occurs naturally in many plants, especially in grapes [32]. The TA is polar due to the presence of polar protic alcohol and carboxylic acid functional groups. In addition, TA was used in the LCB pretreatment process, such as mild organic acid (1 wt% TA) pretreatment of sunflower straw showed promising results with high reducing sugar (RS) recovery and less carbohydrate loss [33]. Organic acids such as TA are derived from biomass and do not cause significant corrosion as they are less acidic than inorganic acids [15]. Thus, to assess the effect of NADES on LCB fractionation, NADES was synthesized

using natural reagents choline chloride (ChCl) as an HBA and tartaric acid (TA) as an HBD in the present work. The properties of NADES-ChCl/TA in their pure form could be very viscous, which can limit its application in LCB pretreatment. The addition of water to NADES-ChCl/TA significantly reduces its viscosity and increases polarity and fluidity [34]. By employing DES in combination with water, the cost of utilizing DES as a bulk solvent in biorefinery can be reduced [35]. Also, the NADES-ChCl/TA in combination with water could result in mild pretreatment conditions. Therefore, the NADES was used for rice straw pretreatment for lignin recovery and enhancing enzymatic hydrolysis. The recovered lignin and reducing sugars (RS) were maximized with minimum sugar derivatization products at the optimum condition. The process was optimized using response surface methodology (RSM) considering three process variables temperature, time, and NADES-concentration, respectively. To further understand the pretreatment mechanism, the compositional changes of rice straw during pretreatment were studied using ATR/FT-IR and PXRD analysis. The recovered lignin was also analyzed by ATR/FT-IR and ¹H-NMR. Also, the feasibility of NADES recovery and its recyclability was investigated.

2 Materials and method

2.1 Materials

The rice straw biomass used in the study was obtained from a paddy agriculture field near the Indian Institute of Technology Hyderabad. The dried rice straw biomass was chopped and ground using a mixer grinder (Prestige Stylo Mixture Grinder). Rice straw biomass was sieved using 30 mesh size (600 micron) to maintain uniform size, and it was kept at room temperature in an airtight container.

2.2 Compositional characterization of rice straw

Rice straw biomass contents (cellulose, hemicellulose, and lignin) were assessed using laboratory analytical procedures (LAPs) for biomass using the NREL technique [36]. The first hydrolysis of the sample was carried out by adding an extractive-free dried rice straw sample (300 mg) in 3 mL of sulfuric acid (H_2SO_4) (72% w/w) at 30 °C for 60 min. Using a vortex shaker, the reaction mixture was shaken every 10 min to keep it homogeneous. After 60 min, deionized water was added to dilute the H_2SO_4 concentration from 72% w/w to 4% w/w in preparation for the second hydrolysis step. For the second hydrolysis, the reaction mixture was autoclaved at 121 °C for 60 min. After the second hydrolysis was complete, the solid residue and liquid hydrolysate were separated using vacuum filtration. The solid waste was kept

in a hot air oven for 12 h to dry. The sample was kept in the muffle furnace for 4 h at 575 ± 25 °C. The ash percentage was found by weighing the solid substance left over from the muffle furnace. The acid-insoluble lignin (AIL) was calculated considering the ash content. The filtrate obtained was analyzed for monosaccharides using ion chromatography (model: Metrohm). Also, the acid-soluble lignin (ASL) was determined using UV–Vis spectrophotometers at a wavelength of 278 nm.

2.3 DES synthesis

The deep eutectic solvent (DES) is synthesized by mixing choline chloride (ChCl) as hydrogen bond acceptor (HBA) and tartaric acid (TA) as hydrogen bond donor (HBD) at the composition of molar ratio at 1:4, respectively. The DES mixture was heated at 80 °C in an oil bath with steady stirring for 4 h until a homogenous, colorless liquid was formed as reported earlier [37]. The prepared NADES-ChCl/TA was then cooled to room temperature and used for the rice straw pretreatment process.

2.4 Design of experiments by response surface methodology (RSM)

The central composite design (CCD) model of RSM was used to design the experimental conditions. The optimal condition was determined using Design-Expert 13. The objective of the experimental design was to maximize the recovery of RS and lignin while minimizing the generation of sugar-derivative compounds. The factors considered for the pretreatment of rice straw were temperature (X_1, °C), time (X_2, min), and DES concentration (X_3, v/v%). The experimental levels of process variables are shown in Table 1. The three-factor experimental design in which 20 runs were conducted is shown in Table S1.

Here low, center, and high levels were set at -1, 0, and $+1$ to improve design resolution and experiment duplicability. The axial points $-\alpha$ and $+\alpha$ with values -1.68 and $+1.68$ were added to predict the function outside the cubic domain. The distance α is defined by $2^{k/4}$, where k is the number of factors. Equation (1) shows a second-order polynomial equation used to fit the experimental dataset. The equation establishes the relationship between the main operating terms, interaction effects, and the predicted responses.

$$R = \gamma 0 + \sum_{i=1}^{k} \gamma i X i + \sum_{i=1}^{k} \gamma i i X i i 2 + \sum \sum_{i<j=1}^{k} \gamma i j X i X_j \qquad (1)$$

where R is the response variable for RS, furan compounds (F), and soluble lignin percentage (L), respectively. X_i and X_j are independent variables. The terms, γ_i, γ_{ii}, and γ_{ij} are model constant, linear coefficient, quadratic coefficient, and interaction coefficient, respectively.

The experimental design and the observed values of 20 experiments are presented in Table S1. The results of 20 experiments were collected in the form of three responses as objectives to optimize the condition of NADES-ChCl/TA pretreatment of rice straw biomass.

2.5 Pretreatment using a high-pressure batch reactor and subsequent DES recovery

The validation of RSM optimal conditions was performed in a 2000 mL non-stirred autoclave with a minimum working amount of 200 mL (make: nano-mag). The batch reactor was purged with nitrogen (N_2) gas for sufficient duration to generate an inert environment, keeping a pressure of 15 bar. The RSM obtained optimal conditions were set. The reactor was cooled immediately after pretreatment, and the equipment was disassembled to quickly remove the reaction tube and stop any further reactions. The reaction mixture was then added with a mixture of acetone and deionized water in a 1:1 ratio, with the volume of the solution being three times that of the reaction mixture. The mixture was stirred for 30 min to ensure complete dissolution of lignin. After vacuum filtration, the resulting black liquor was transferred to a 500-mL beaker. The solid residue (pretreated rice straw) was then washed with water to remove the remanence of NADES. After the washing step, the pretreated rice straw biomass was dried at a temperature of 104 °C for 4 h and kept in an airtight container before enzymatic hydrolysis. The liquid hydrolysate was diluted three times with deionized water and left to settle at room temperature for 12 h for lignin precipitation. The liquor was centrifuged for 10 min at a speed of 4000 rpm to separate the lignin. The solid leftover in the centrifuge tube after decantation was kept for drying for 12 h at 60 °C to obtain solid dry lignin.

Table 1 Experimental levels of process variables in the CCD model

Variable	Code	$-\alpha$	-1	0	$+1$	$+\alpha$
Temperature (°C)	X_1	81.00	96	118	140	154.99
Pretreatment time (min)	X_2	72.72	100	140	180	207.27
DES concentration (v/v%)	X_3	5.14	14	27	40	48.86

The resultant brown-colored powder was the recovered lignin, and its yield was estimated by using Eq. (2). The DES was recycled from the liquid hydrolysate comprised of water and DES. After lignin precipitation, the DES-water mixture solution was evaporated at 70 °C under reduced vapor pressure using a rotatory evaporator to recover the DES. The DES was collected in the round-bottomed flask as dark viscous leftover liquid with traces of sugars and lignin.

$$\text{Lignin recovery}, \% = \frac{\text{Recovered Lignin after pretreatment, g}}{\text{Lignin in rice straw, g}} \times 100 \tag{2}$$

2.6 Quantification of sugar, furan, and soluble lignin

2.6.1 Sugar analysis

Ion chromatography was used to determine the contents of monosaccharides present in the liquid hydrolysate (filtrate or black solution after filtration). An amperometric detector was used for detecting the monosaccharides present in the pretreated hydrolysate and enzymatic hydrolysate. The column used was Hamilton RCX-30–250/4.6 (make: Metrohm) with a column oven temperature of 32 °C. The injection volume was 20 μL. The mobile phase (0.75 mM NaOH) flow rate was set to 1 mL/min. To determine the concentrations of sugars in unknown samples, standard calibration curves for arabinose, galactose, glucose, xylose, and mannose were generated.

2.6.2 Furan analysis

The RS degradation compounds (5-hydroxymethylfurfural and furfural) were quantified using LC-DAD. The quantification of these furan compounds was done using LC-DAD (model: 1260 Infinity II, Make: Agilent Technologies, USA). The compounds are eluted using Zorbax Eclipse Plus C18 (2.1×50 mm, 1.8-micron particle size) as an analytical column. The mobile phase used for the elution of furan compounds was 80% methanol (99.99% HPLC grade) in 20% HPLC grade water in an isocratic mode with a flow rate of 0.12 mL/min. The compounds were detected at 280 nm wavelength. The column oven temperature was set at 30 °C. Using the standard calibration curve, the levels of furan compounds in the hydrolysate were determined.

2.6.3 Soluble lignin analysis

The quantification of lignin monomer in the liquid hydrolysate was performed using an Agilent LC–MS system with Q-TOF (model: 1260 Infinity II, make: Agilent) mass spectrometry in positive mode. The separation of lignin monomers was performed on a Zorbax Eclipse Plus C18 (2.1×100 mm, 1.8-micron particle size) column at a column temperature of 30 °C. The mobile phases were (A) 0.1% formic acid (99.9%, LC–MS grade) in LC–MS grade water and (B) methanol (99.99%, LC–MS grade). The mobile phase flow rate was 0.1 mL/min. The lignin monomers were eluted with gradients (i) 0–3 min (A, 100%; B, 0%), (ii) 3–6 min (A, 20%; B, 80%), (iii) 6–9 min (A, 80%; B, 20%), and (iv) 9–12 min (A, 20%; B, 80%) maintaining (A, 100%; B, 0%) in 12th min of gradient flow mobile phase at 0.10 mL/min. The sample injection, nebulizer pressure sheath gas temperature, gas temperature, drying gas flow, capillary voltage (V_{cap}), and nozzle voltage were 10 μL, 45 psi, 350 °C, 250 °C, 11 L/min, 3500 V, and 1000 V, respectively. The MS TOF fragment or voltage was 185 V with a skimmer of 75 V. The standard calibration curve for lignin monomers was made with the MassHunter Quantitative software from Agilent Technologies with different levels of prepared lignin monomers mixed standards.

2.7 FTIR characterization

Fourier transform infrared (FTIR) spectroscopy was conducted in a wavelength range of 4000 to 600 cm^{-1} with a resolution of 4 cm^{-1} in attenuated total reflection (ATR) mode. In the Bruker ATR-FTIR device, the different samples were examined to characterize NADES-ChCl/TA in terms of the raw material, isolated lignin, and untreated and pretreated rice straw biomass. The change in molecular order can be assessed by comparing marker peaks in the ATR-FTIR spectra of the untreated and pretreated rice straw biomass. The hydrogen bonding index (HBI) can be calculated from the absorbance ratio at 3350 and 1337 cm^{-1}. The HBI offers information associated with the extent of hydrogen bonding. Generally, it is determined to observe variations in the hydroxyl groups present in the cellulose structure. The total crystallinity index (TCI) is determined from the absorption ratio of O–H bending vibration (1373 cm^{-1}) and C-H stretching vibration (2900 cm^{-1}). The TCI is examined to ascertain cellulose crystallinity, as TCI is directly correlated with the degree of cellulose crystallinity [38]. The change in molecular ordering can be assessed using the lateral order index (LOI). The HBI, total crystallinity index (TCI), and lateral order index (LOI) were determined using the following equations (Eqs. (3)–(5)) [39]:

$$\text{HBI} = \frac{A_{3350\text{cm}^{-1}}}{A_{1337\text{cm}^{-1}}} \tag{3}$$

$$\text{TCI} = \frac{A_{1373\text{cm}^{-1}}}{A_{2900\text{cm}^{-1}}} \tag{4}$$

$$LOI = \frac{A_{1427\text{cm}^{-1}}}{A_{895\text{cm}^{-1}}} \qquad (5)$$

2.8 Thermal properties

The thermal properties of NADES-ChCl/TA were analyzed using differential scanning calorimetry (DSC; make: TA Instruments, model: DSCQ200). The experiment was conducted from 25 to 400 °C, with a temperature step of 5 °C/min, under an inert N_2 atmosphere.

2.9 *^{1}H-NMR characterization*

Nuclear magnetic resonance (NMR) spectroscopy was used to study the different environments of protons present in recovered lignin. ^{1}H-NMR and two-dimensional heteronuclear singular quantum correlation (2D HSQC) NMR spectra were obtained on a 400 MHz spectrometer (Bruker Advance II) at 298 K. The lignin sample weighing 30 mg was dissolved in 600 µL of dimethylsulfoxide-d_6 (DMSO-d_6) within Teflon tape-sealed vials and kept for sonication below 50 °C. The chemical changes were referenced to the primary peak of DMSO-d_6 (δ_H 2.5 ppm). MestReNova software, version 6.0.2–5475, was utilized for peak assignment and calculation of area integrals.

2.10 X-ray diffraction (XRD) analysis

The raw and pretreated rice straw samples were examined for XRD using a PANalytical Empyrean diffractometer (Cu-$K\alpha_1$ radiation 1.5405498 Å). As a control, the XRD pattern of untreated rice straw biomass was used. The analysis was carried out at 45 kV and 40 mA using a 1.54 nm wavelength with a step size of 0.0131° in the 2θ range between 5 and 90°. XRD evaluation was carried out

to determine the crystallinity index (CrI) of the raw and pretreated rice straw sample by Eq. (6) [40].

$$CrI = \frac{I_{200} - I_{am}}{I_{200}} \times 100 \qquad (6)$$

where I_{200} and I_{am} are the peak intensities at 2θ of 22° and 18°, respectively [41]. The straight line between 5 and 90° was considered as a baseline to which the intensity data was calculated.

2.11 Enzymatic hydrolysis

Under sterilized conditions, 400 mg of raw and DES-ChCl/TA pretreated rice straw was added to sodium citrate buffer (50 mM, pH 4.8). The enzymatic saccharification was carried out by using commercial enzymes, such as cellulase (C1794, make: Sigma-Aldrich, USA) and β-glucosidase enzymes (G0395, make: Sigma-Aldrich, USA), having enzymatic activity of 5.1 cellobiase units (CBU)/g and 97 filter paper units (FPU)/mL, respectively [10, 35]. For this study, the mixture of enzymes in the apparatus contains 10 CBU β-glucosidase and 15 FPU cellulase per gram of dry substrate. The enzymatic hydrolysis was carried out in a rotary shaker incubator (model: Remi) set at 150 rpm at 50 °C for 144 h using a 50-mL Erlenmeyer flask. Tween 80 (0.1%) was added to enhance enzymatic digestion, and sodium azide (NaN$_3$, 0.3%) was added for the prevention of microbial growth. The total reaction medium volume was 20 mL. The samples were collected at regular intervals of 24 h and boiled at 95 °C in a water bath for at least 5 min to deactivate the enzymatic reaction, following which they were vacuum filtered. The concentration of RS was determined by ion chromatography. Enzymatic hydrolysis of raw and DES-ChCl/TA pretreated rice straw was carried out simultaneously, and the results were compared. All tests were carried out in triplicate to reduce the experimental error. The fermentable sugar yield was calculated using Eq. (7):

$$RS \text{ yield } (\%) = \frac{(RS \text{ released}(\frac{\text{mg}}{\text{L}}).V_{\text{hydrolysis}}(\text{L}))}{A \text{ mass of rice strawhydrolyzed (mg). Total sugars in pretreated rice straw (\%)}}.100 \qquad (7)$$

3 Results and discussion

3.1 Rice straw composition

The rice straw biomass contains $31.75 \pm 3.09\%$ cellulose, $14.70 \pm 1.07\%$ hemicellulose, $2.22 \pm 0.39\%$ ASL, and $14.90 \pm 0.26\%$ AIL. Total lignin was observed to be $17.12 \pm 0.65\%$ and an ash content of $9.40 \pm 0.44\%$. The composition of rice straw in this study was in agreement with the rice straw batches reported elsewhere. For

instance, Sawhney et al. reported 17.85% hemicellulose and 34.88% cellulose in raw rice straw biomass [42]. Similarly, Sorn et al. reported that untreated rice straw consists of lignin ($20.00 \pm 0.44\%$), hemicellulose ($15.73 \pm 0.31\%$), and cellulose ($30.88 \pm 0.39\%$) [43]. Likewise, Singh et al. reported untreated rice straw with a composition of 43% cellulose, 23% hemicellulose, 10.2% lignin, and 18.8% ash [44]. Kumar et al. also observed cellulose, hemicelluloses, and lignin content of 35.5%, 25.6%, and 16% as major components in rice straw biomass [45]. The composition
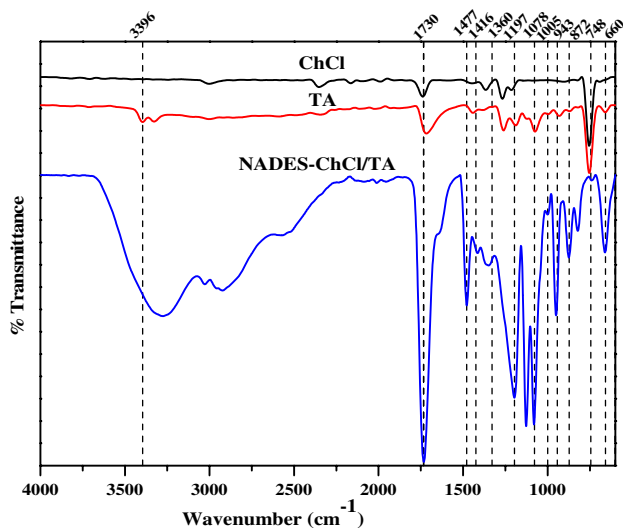
Fig. 2 ATR-FTIR characterization of NADES-ChCl/TA

Fig. 3 DSC plot of NADES-ChCl/TA

of rice straw biomass changes with the region. The minor deviations in the rice straw components may be attributed to factors like climate, cultivation conditions, location, and types of rice straw [46].

3.2 ATR-FTIR characterization of NADES-ChCl/TA

The driving force for the formation of DES is the hydrogen bonding between the chloride anion of HBA (ChCl) and HBD (tartaric acid). Figure 2 represents the ATR-FTIR spectra of ChCl, TA, and ChCl: TA. The FT-IR spectra show that the stretching vibration of the O–H functional group first observed at 3396 and 3326 cm^{-1} in TA has broadband occurrence in between 3200 and 3500 cm^{-1} in NADES-ChCl/TA DES. The broadness and shifting of peaks were due to the incorporation of ChCl and TA by forming more hydrogen bonding with the decrease in the extent of intermolecular hydrogen bonding between TA molecules [47]. The band at 2921 cm^{-1} and 2990 cm^{-1} is due to Sp^3 C-H stretching vibration contributed by ChCl and TA. The carbonyl stretching vibration is attributed to the occurrence of the strong peak at 1730 cm^{-1} in the NADES-ChCl/TA spectra [48]. The strong band at 1477 cm^{-1} and 1416 cm^{-1} is due to the CH_2 and CH_3 moieties bending vibration in the NADES-ChCl/TA. The band at 1078 cm^{-1} and 1005 cm^{-1} was due to C-O and C–C-O stretching, respectively. The additional band at 943 cm^{-1} is attributed to the C-N^+ stretching vibration. The C-N^+ symmetric stretching of ChCl was also detected at 748 cm^{-1} [49]. The C-H bending vibration of TA caused the band at ~748 [50]. The components of NADES-ChCl/TA were combined by hydrogen bonding. There will be a strong
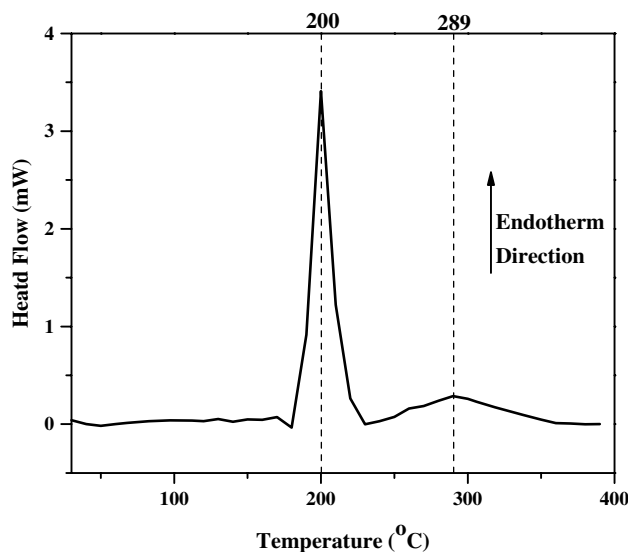
intermolecular interaction among the protons of ChCl and TA in NADES-ChCl/TA [51]. Also, the cationic center will interact with oxygen, being a more electronegative atom of TA. Thus, the band at ~748 in the pure form of the NADES-ChCl/TA components has been obstructed, causing the fading of the band in NADES-ChCl/TA spectra. However, a weak band was discernible with a shift toward lower wavenumber (~748 cm^{-1}) in NADES-ChCl/TA spectra, which could be due to the preservation of the C-N^+ functional group in the resultant NADES-ChCl/TA. The band at 660 cm^{-1} originates due to the out-of-plane wagging vibration of C-O–H in NADES-ChCl/TA [52, 53]. Thus, the synthesized NADES-ChCl/TA was characterized with ATR-FTIR to observe the bands corresponding to different functional groups.

3.3 Thermal properties of NADES-ChCl/TA

The NADES-ChCl/TA in the present study was formed with a 1:4 ratio of ChCl and TA. The DSC endotherm peak temperatures for NADES-ChCl/TA have degradation temperatures at about 200 and 289 °C which could be attributed to the degradation temperature of ChCl and TA, respectively (Fig. 3). Similar observation has been reported by Koutsoukos et al. during the DSC and TGA analysis of NADES-ChCl/TA (2:1 ratio) where the degradation temperatures of TA and ChCl were at about 220 and 280 °C, respectively [51]. The NADES-ChCl thermal properties may vary from that of the ChCl and TA in their pure form due to the formation of a dense hydrogen bonding network in NADES-ChCl/TA [51]. Thus, the formation of the NADES-ChCl/TA with the DSC spectra resembles the work that was reported; the DES-ChCl/TA system requires

more energy for degradation. The more energy required can be for the cause of hydrogen bonding network disruption.

3.4 Optimization of pretreatment condition for maximum glucose and lignin yield

The optimization of process variables was done based on RSM, using Design-Expert 13. The responses considered were the percentage RS, furan compounds, and lignin. The responses have been expressed in terms of second-order equations (Eqs. (8)–(10)).

$$
\begin{aligned}
RS_1 = {} & -710.5 + 8.353X_1 + 2.926X_2 + 5.023X_3 \\
& - 0.02698X_1X_1 - 0.007436X_2X_2 - 0.02219X_3X_3 \quad (8) \\
& - 0.007571X_1X_2 - 0.03188X_1X_3 + 0.00004X_3
\end{aligned}
$$

$$
\begin{aligned}
F_1 = {} & 183.0 - 2.713X_1 - 0.5296X_2 - 0.139X_3 \\
& + 0.011684X_1X_1 + 0.001674X_2X_2 + 0.02807X_3X_3 \quad (9) \\
& - 0.001615X_1X_2 - 0.0026X_1X_3 - 0.004708X_2X_3
\end{aligned}
$$

$$
\begin{aligned}
L_1 = {} & -125.26 + 1.5984X_1 + 0.5157X_2 + 0.5356X_3 \\
& - 0.006234X_1X_1 - 0.001511X_2X_2 - 0.007673X_3X_3 \quad (10) \\
& - 0.000765X_1X_2 - 0.001036X_1X_3 - 0.000118X_2X_3
\end{aligned}
$$

where RS_1 is the response (RS yield), F_1 is the response (furan compounds), L_1 is the response (soluble lignin yield), X_1 is the temperature, X_2 is the time, and X_3 is the NADES-ChCl/TA concentration. The response behavior is described by a mathematical equation as a function of the independent variables. The effectiveness of the model was evaluated using analysis of variance (ANOVA). Table S2 displays ANOVA results for all three responses. The ANOVA results demonstrated that the model was statistically significant by a p-value less than 0.05, whereas lack of fit was not significant with a p-value greater than 0.05 for all three responses. The coefficient of determination (R^2) with values 0.99 for all

three responses indicates that there is a very good correlation between experimental and predicted ones. The adjusted coefficient of determination for the three responses is 0.98, 0.99, and 0.98 for RS_1, F_1, and L_1, respectively, confirming that the model adequately predicted the responses. Also, the value of predicted R^2 for the three responses is 0.94, 0.97, and 0.96 for RS_1, F_1, and L_1, respectively. The model summary in this study where R^2 and the modified R^2 were > 0.8 indicates that the model performed satisfactorily [54]. The predicted vs observed plot (Fig. 4) was utilized to verify the validity of the developed method and the correlation between the observed and expected results. The analysis of predicted and observed responses showed very close agreement between them as both the points lie very near to the straight line. This showed that the method was designed well and reliable [42]. Thus, the second-order model successfully predicts the response since the predicted and observed values are very close to one another.

3.5 Effect of variables on response

The 3D surface plots accompanying contour plots illustrate the influence of each variable and the approximate optimal location. In 20 experimental runs, the varied response (RS_1, 12.52–57.86; F_1, 0.82–24.95; and L_1, 1.94–9.10) shows the impact of the variable in different levels (Table S1). The observation of the experiment to optimize the process was also studied using the response surface plot shown in Fig. 5. The interactions of process variables for three different responses were observed using the surface plot.

3.5.1 Time, temperature, and NADES-ChCl/TA concentration interactions on RS release

The interactive effect of time, temperature, and concentration on RS release from rice straw was illustrated using Fig. 5a–c. The response plot in Fig. 5a displays the range
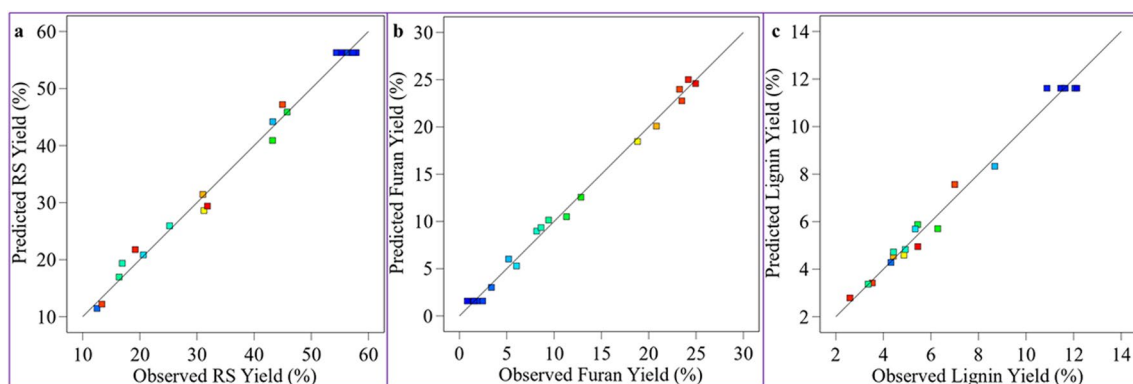

Fig. 4 Predicted vs actual plot of **a** RS, **b** furan compounds, and **c** lignin yield on NADES-ChCl/TA pretreatment
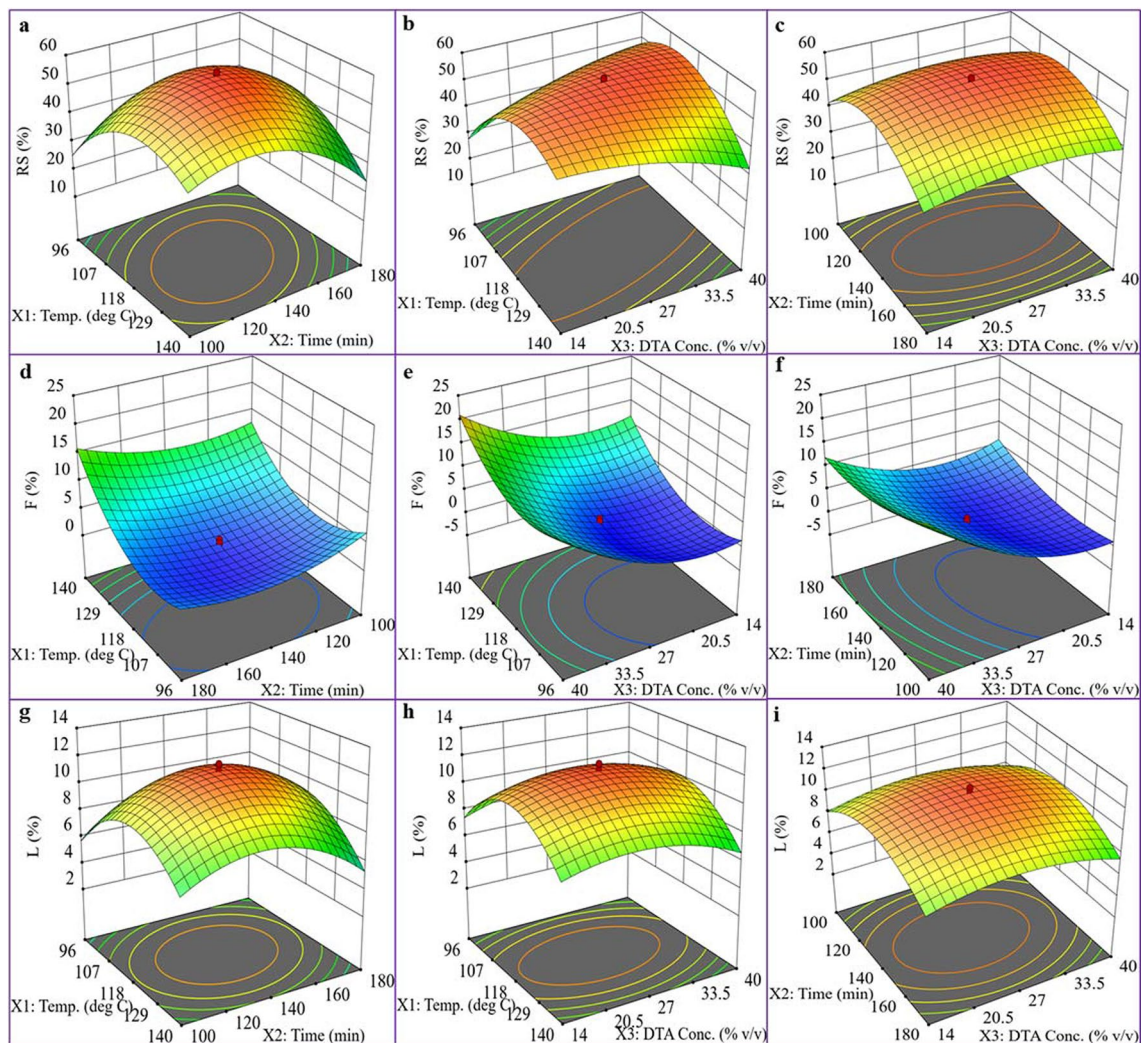
Fig. 5 3D response surface plot for the effect of pretreatment temperature, DTA conc. (NADES-ChCl/TA concentration), RS recovery (**a–c**), furan compound yield (**d–f**), and lignin yield (**g–i**) for NADES-1 pretreatment

of temperatures (107–129 °C) and pretreatment time (110–150 min) over which the yield of RS recovery varied from 45 to 55%. It was observed around the above-mentioned region as the highlighted surface plot along with the contour plot at the bottom also depicts the optimal region where the experiment can be performed. At the optimum condition, the maximum amount of RS recovery (56%) was observed at 117.63 °C and 137.96 min. The higher amount of RS is recovered at this condition because of the high amount of solubilization of carbohydrates and lignin resulting in disruption of rice straw biomass structure. In Fig. 5b, low temperature and NADES-ChCl/TA concentration gave comparatively little effect on RS yield; however, as temperature and NADES-ChCl/TA concentration rise, the RS yield has also increased. The optimal range of NADES-ChCl/TA concentration for this rise in RS yield was somewhere in the middle. This is because the hydrogen bonds between

cellulosic polymers are being broken down as additional hydrogen bonding forms between the NADES-ChCl/TA and the carbohydrate-lignin matrix [55]. Therefore, removing lignin and xylan along with the structural modification of cellulose results in a higher RS yield [56]. In Fig. 5c, we can see how the RS recovery changes over time and as a function of NADES-ChCl/TA concentration when the temperature is held constant at the midpoint (118 °C). The short period of pretreatment time yields less recovery of RS, but as time increases, there is a rise in RS yield, and after a certain threshold, there is a decline in the RS yield. This drop in RS recovery could be due to the solubilization of released cellulose with prolonged pretreatment time [57]. The NADES-ChCl/TA concentration also affects RS recovery as shown in Fig. 5c; the NADES-ChCl/TA concentration in the mid-range (25 to 35 w/w%) interaction with time resulted in the maximum condition for RS yield which is represented by the

highlighted region of the surface plot. The yield of RS was adversely affected by extreme, too high, or low temperature and concentration, as well as by prolonged and short pretreatment time. The extreme pretreatment conditions are too harsh, and the cellulose becomes soluble to produce sugar derivative compounds like furfural and 5-HMF [58]. These sugar derivative compounds inhibit the further downstream process such as enzymatic hydrolysis and fermentation. The components of rice straw cannot be depolymerized effectively at too low temperature and concentration for a shorter pretreatment time. Thus, in this study, the optimization of process parameters (temperature, pretreatment time, and NADES-ChCl/TA concentration) is acquired for maximum recovery of RS from the rice straw biomass.

3.5.2 Time, temperature, and NADES-ChCl/TA concentration interactions on lignin release

The interactions between process variables and lignin solubility are represented in Fig. 5 g–i. It was found that the soluble lignin yield was low at lower temperatures. The dome shape surface plot as shown in Fig. 5g depicts low temperature and less treatment time yielding lesser lignin recovery, but it rises with both parameters. The highest lignin recovery occurs in the center of the contour plot (around 118 °C and 140 min), and after a certain point, it decreases significantly. The acceleration of lignin yield at elevated temperatures was previously reported [59, 60]. Poy et al. also observed a similar trend with maximum delignification (64.9%) from rice straw pretreatment with 1-ethyl-3-methylimidazolium acetate at an optimized condition of 120 °C for 5 h [61]. Figure 5h also displays the highlighted surface plot with maximum lignin recovery at around 118 °C and 28% NADES-ChCl/TA concentration supported by the contour plot at the bottom. The lesser pretreatment time with low DES concentration has less impact on the lignin recovery (Fig. 5h). In the present study, it was observed that with an increase in temperature, there was enhanced lignin recovery. The increase in the solubility of rice straw biomass with the decrease in viscosity of NADES-ChCl/TA at higher temperatures results in maximum lignin recovery. The DES viscosity decreases with the increase in temperature leading to a high degree of LCB dissolution [62]. Thus, the lignin recovery was highly influenced by the increase in temperature and NADES-ChCl/TA concentration. The interaction

effect of NADES-ChCl/TA concentration and time for lignin recovery is represented in Fig. 5i. The surface plot highlighted by the red color region with a contour plot circled by the same color at the bottom depicts the area where the optimum pretreatment condition can be found. The disruption of the molecular structure of the lignin-carbohydrate complex at optimum conditions leads to higher lignin recovery. This may be due to the depolymerization of lignin by cleavage of bonds such as β-O-4 ether linkages during the NADES-ChCl/TA pretreatment process [43, 63]. Thus, the present study shows more interaction of NADES-ChCl/TA with the natural system present in rice straw biomass to produce the maximum lignin at the optimum condition of the designed process parameters.

3.5.3 Time, temperature, and NADES-ChCl/TA concentration interactions on furan compound release

During the process optimization of NADES-ChCl/TA pretreatment of rice straw, the formation of furan compounds such as furfural and 5-hydroxymethylfurfural (5-HMF) was investigated. Figure 5d–f shows the interaction effect of the process variables on the generation of furan compounds. The temperature–time interaction effect in the furan compound formation is depicted in Fig. 5d. The NADES-ChCl/TA concentration was kept constant at the center (40%); Fig. 5d illustrates the reactivity of the furan compound variation over time and temperature. The optimal condition with minimum production of furan compound was observed at the temperature of around 118 °C and 140 min pretreatment time. When there is a rise in temperature with prolonged heating, more C_5 and C_6 sugars will be converted into their derivative compounds [64, 65]. The surface plot in Fig. 5d depicts a similar trend, and there was an increase in the furan compound yield with the rise in temperature and time. The temperature and NADES-ChCl/TA concentration impact was observed with the surface plot shown in Fig. 5e. A lower temperature and less concentration of NADES-ChCl/TA during pretreatment yield limited furan compounds, but the increase in temperature and NADES-ChCl/TA concentration generates more furan compounds (Fig. 5e). This may be due to the generation of harsh reaction conditions in the extreme case of process variables [64].

Table 2 Predicted and observed responses for NADES-ChCl/TA at optimized pretreatment conditions

| Case	Temperature (X_1)	Time (X_2)	NADES-ChCl/TA concentration (X_3)	RS %		Furan compounds %		Soluble lignin %	
				Pred	Exp	Pred	Exp	Pred	Exp
NADES-ChCl/TA	117.63	137.96	25.01	56.08	57.11 ± 1.43	0.78	1.15 ± 0.28	11.61	12.58 ± 0.23

The NADES-ChCl/TA also acts as a catalyst during the pretreatment, but the higher concentration of NADES-ChCl/TA at elevated temperatures results in harsh reaction conditions resulting in the production of more furan compounds [66]. The interaction effect of time and NADES-ChCl/TA concentration is observed in Fig. 5f. In this case, also taking two variables and with temperature constant at the center point (118 °C) shows a similar trend as mentioned above. As the level of process variables increased, furan compound yield decreased, but after minimum yield, it ascended again toward the extreme level of the process variable. The generation of furan compounds in the present study was minimized as these compounds are also known as inhibitory chemicals. Furan compounds hinder further downstream processes such as enzymatic hydrolysis and yeast growth during the fermentation. The process was optimized as predicted values presented in Table 2 for maximum recovery of RS (56.08%) and lignin (11.61%) with minimum production of furan compounds (0.78%). The observation based on the interaction of

process variables in the current study offers the best condition of the experiment within the selected range. Also, the optimal condition of NADES-ChCl/TA pretreatment of rice straw biomass falls in the range of the variables. Thus, in the present study, process parameters were optimized to enhance RS and lignin recovery while reducing the generation of furan compounds.

3.6 Characterization optimum condition liquid hydrolysate

The effect of NADES-ChCl/TA on the rice straw pretreatment was analyzed based on biomass fractionation. The liquid hydrolysate collected at optimum conditions was analyzed for different contents of RS, lignin monomers, and furan compounds. The optimal values for the independent variables, along with the predicted and observed response values, are shown in Table 2. The experiments were conducted in triplicate to verify the model-obtained results. The RS, furan compound, and soluble lignin yields

Fig. 6 The liquid hydrolysate profile **a** RS, **b** lignin monomers, and **c** furan compounds
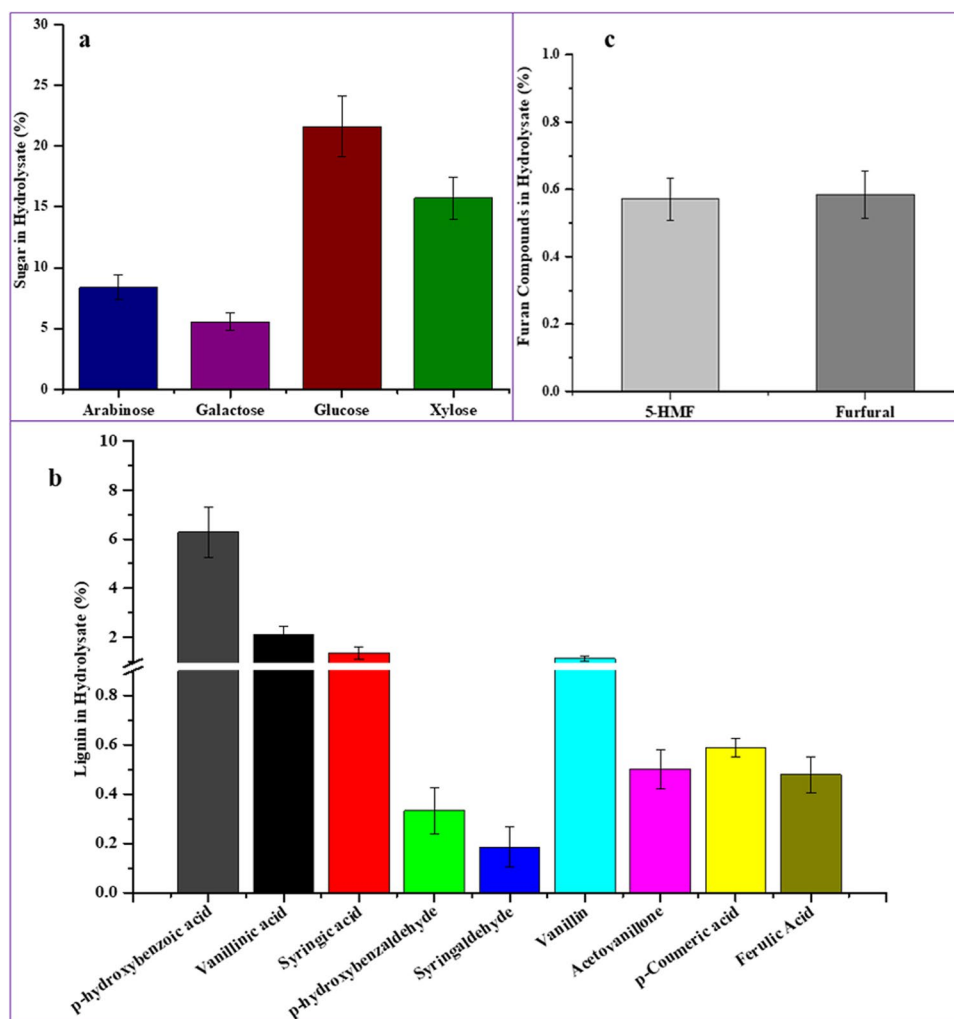
obtained under optimum condition experimental run were $57.11 \pm 1.43\%$, $1.15 \pm 0.28\%$, and $12.58 \pm 0.23\%$ which are very near to the model predicted value of 56%, 0.78%, and 8.76%, demonstrating the accuracy of the model.

The composition of different monosaccharides (RS) observed in the liquid hydrolysate is shown in Fig. 6. The recovery RS comprises $21.61 \pm 5.51\%$ glucose yield with other sugar monomers following pretreatment using NADES-ChCl/TA. As shown in Fig. 6a, the high recovery of glucose followed by xylose provides insight into the mechanism and effect of NADES-ChCl/TA on the composition of rice straw. The rice straw biomass in the present study was composed of cellulose in a higher fraction compared to hemicellulose. Thus, during NADES-ChCl/TA pretreatment, the high portion of cellulosic polymers on exposure to NADES cleaves more of the β-1,4-glycosidic bond resulting in high glucose recovery. The NADES-ChCl/TA pretreatment shows the higher solubilization of RS present in rice straw, and it is necessary to determine the extent of lignin monomer solubilization in NADES pretreatment. The observation of different lignin monomers present in the hydrolysate is shown in Fig. 6b. The different lignin monomers are identified as p-hydroxybenzoic acid, vanillic acid, syringic acid, p-hydroxybenzaldehyde, syringaldehyde, vanillin, acetovanillone, coumaric acid, and ferulic acid. The molecular structure of lignin is composed of different lignin monomers bonded with diverse orders of chemical bonds [67]. Lignin monomers and their derivatives are formed when the β-O-4 aryl ether link is broken during pretreatment [68]. Lignin is composed of various aromatic subunits, including the p-hydroxyphenyl type (H), guaiacyl type (G), and syringyl type (S). These three types of phenylpropane units, also known as monolignols, are regarded to constitute the main constituents of lignin [69]. The total number of methoxy groups that are bonded to an aromatic ring differentiates the monolignols from one another [70]. Lignin H-type derivatives include monomers like p-hydroxybenzoic acid, p-hydroxybenzaldehyde, and p-coumaric acid. The G-type monomers include vanillin, vanillic acid, ferulic acid, and acetovanillone whereas the S-type includes syringaldehyde and syringic acid. In terms of the soluble lignin monomers, liquid hydrolysate has a relatively higher percentage of p-hydroxybenzoic acid $(6.28 \pm 1.01\%)$ than vanillic acid (2.09 ± 0.36) and syringic acid $(1.36 \pm 0.0.26)$.

There have been several investigations into the potential of DES pretreatment to improve enzymatic hydrolysis and lignin recovery. For instance, Xu et al. reported the lignin extraction of ~10% at 160 °C from corn stover during ChCl/Gly (1:2) pretreatment [71]. Similarly, Guo et al. found 63.10% lignin removal during the DES (benzyltriethylammonium chloride (BTEAC)/lactic acid (LA), 1:2) pretreatment of corncob at 140 °C [72]. Likewise, Chen et al.

showed a lignin removal of 47.10% in DES (betaine/LA) pretreatment of sugarcane bagasse at 160 °C for 80 min [73]. According to Pan et al., the DES pretreatment of rice straw biomass observed acid-insoluble lignin hemicellulose and cellulose of 22.87%, 16.71%, and 9.60% at the optimum condition at 130 °C for 4 h [55]. Similarly, Maibam et. al. investigated DES-ChCl/acetic acid (AA) pretreatment of rice straw pretreatment at 126 °C, 2.5 h, and found 83.1% delignification [37]. Most of the reported studies on DES pretreatment of LCB involve harsh pretreatment conditions aiming to extract lignin and other value-added products. The present study operates on the mild pretreatment condition using highly environmentally benign solvents showing the high recycling efficiency of the NADES-ChCl/TA with the lignin recovery of 45.33 ± 2.02 mg per gram (~27% of total lignin). Furthermore, in comparison to conventional chemical pretreatments such as acid, alkali, and other chemical pretreatments, which have adverse environmental consequences, NADES pretreatment is an eco-friendly alternative.

The sugar degradation compound (furan compounds) profile is shown in Fig. 6c. Due to the inhibitory effects of furan compounds on subsequent processes such as enzymatic hydrolysis and fermentation, their concentrations are kept as low as possible under optimal conditions. The furan compounds are produced around 1.15% which is negligible compared to the RS recovery. Ultimately, this work reflects the importance of NADES-ChCl/TA in the recovery of lignin and sugars from rice straw biomass and the recyclability of the pretreatment solvent. This study additionally demonstrates the production of a low concentration of inhibitory compounds with improved efficiency of the downstream process including enzymatic hydrolysis.
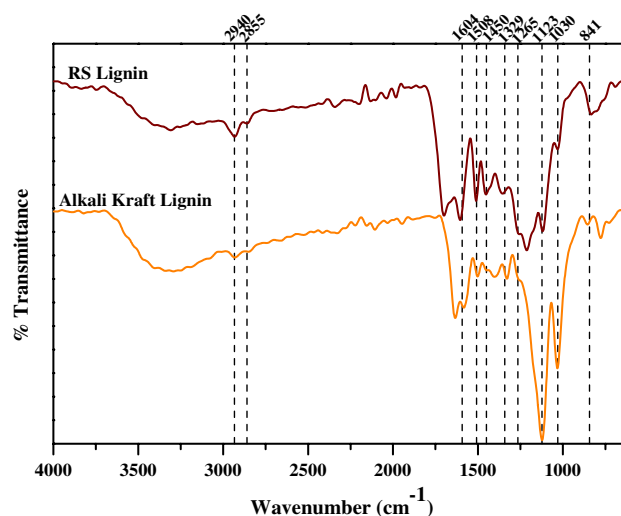

Fig. 7 IR spectrum of isolated lignin of rice straw using NADES-ChCl/TA and commercial alkali kraft lignin

3.7 ATR-FTIR of lignin

ATR-FTIR is used to characterize different functional groups and structural fragments and is a very sensitive and reliable way to study the conformational and physicochemical properties of lignin. Figure 7 represents the comparative ATR-FTIR spectrum of commercial standard alkali kraft lignin and isolated lignin of rice straw with NADES-ChCl/TA pretreatment. The broad absorption band in the region of 3250–3500 cm^{-1} with an intensity peak around 3310 cm^{-1} corresponds to the stretching vibration of -OH bonds, indicating the presence of aromatic and aliphatic -OH functional groups. The peaks in the positions of 2940 and 2855 cm^{-1} are due to stretching vibration of aliphatic methyl (-CH$_2$) and methylene (-CH) side chains as well as chains of aromatic methoxy functional groups [35]. The C-H bending vibration at 1450 cm^{-1} confirms the presence of methyl and methylene groups in the isolated lignin which is similar to that of the commercial alkali kraft lignin (Fig. 7). The strong peak at 1700 cm^{-1} originated from stretching of unconjugated carbonyls of carboxylic acidic groups. The absorption band at 1604 and 1508 cm^{-1} corresponds to the stretching vibration of aromatic carbon–carbon double (C=C) and carbon–carbon single bond (C–C) of lignin molecules [74]. The peaks around 1329 cm^{-1} are attributed to the stretching vibration of C-O attached to syringyl rings. This indicates rice straw lignin contains methoxy groups and has syringyl units [75]. The shoulder peak at 1265 cm^{-1} was due to the C-O stretching vibration of guaiacyl rings displayed in the isolated lignin spectra which are also in agreement with the standard kraft lignin spectra [76]. The absorption bands at 1123 and 1030 cm^{-1} were observed due to aromatic C-H vibration of syringyl and aromatic C-H in-plane deformation of guaiacyl units [77]. Aromatic C-H out-of-plane bending vibration of syringyl and guaiacyl units has a characteristic peak at around 841 cm^{-1} in FTIR spectra of isolated and standard kraft lignin. These bands of guaiacyl and syringyl units show that G and S units are more prevalent in the isolated lignin [77]. The ATR-FTIR spectra of isolated lignin are similar to that of the commercially available alkali kraft lignin. Thus, the lignin extracted from rice straw pretreatment using DES-ChCl/TA as a green solvent produces lignin comparable to the commercially available kraft lignin.

3.8 ^{1}H-NMR of isolated lignin

The isolated lignin from rice straw was characterized by NMR spectroscopy (Fig. 8). The ^{1}H-NMR spectra show large and broad bands for the majority of the protons, which are characteristic of high-molecular-weight polymers with high relaxation time [78]. The peaks in the region of δ_H ~ 0.80–2.30 ppm can be particular for the aliphatic moiety
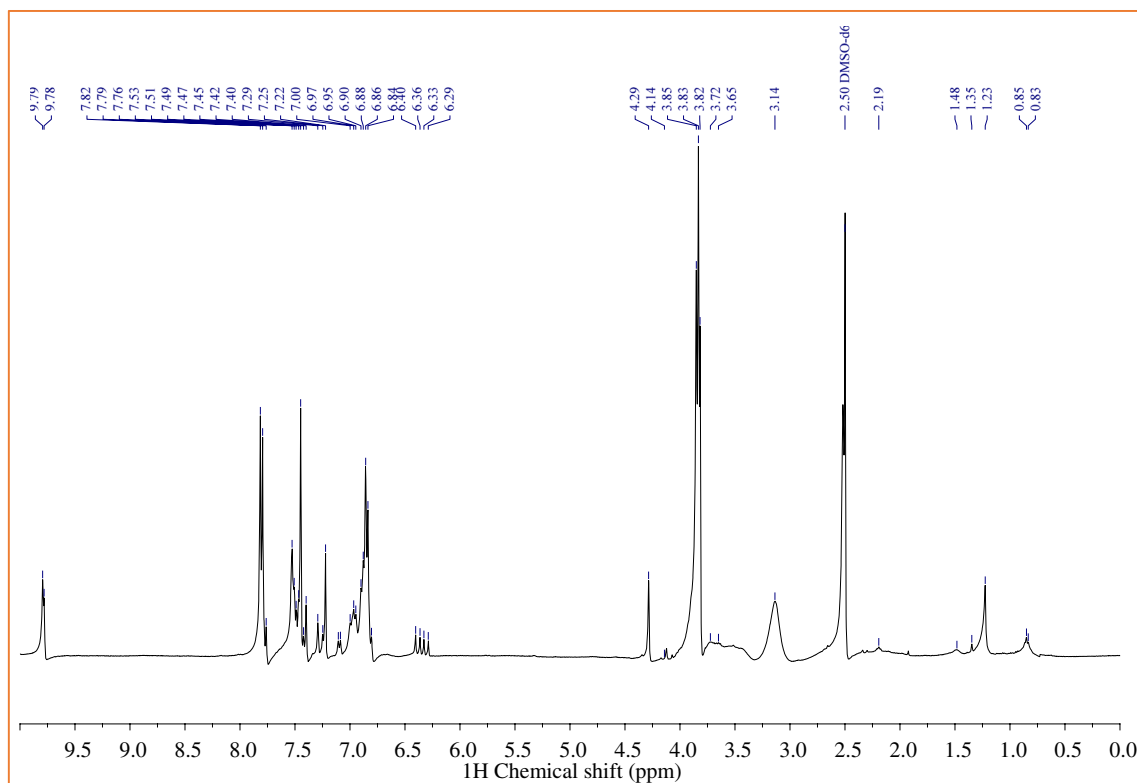

Fig. 8 ^{1}H-NMR extracted lignin by NADES-ChCl/TA

due to aliphatic protons of several methoxy ($-OCH_3$) and methylene ($-CH_2$) groups [79]. The intense peak at 2.50 ppm is due to DMSO-d_6 (dimethyl sulfoxide-d_6) used as an NMR solvent. The broad signal around $\delta_H \sim 3.14$ ppm is attributed to the moisture content in the sample. The presence of moisture in both the sample and solvents contributes to the appearance of the water/moisture contamination signal. The methoxy groups ($-OCH_3$) immediately bonded to the benzene ring which is related to S and G units causing the proton signals at $\delta_H \sim 3.83$ ppm. The peaks originating from the aliphatic side chains of the lignin skeleton are in the region from $\delta_H \sim 4.00–5.50$ ppm. The primary aromatic peak in syringyl proton (S) occurs between $\delta_H \sim 6.10$ and 6.70 ppm whereas the aromatic peak in guaiacyl proton (G) occurs between $\delta_H \sim 6.70$ and 7.50 ppm [80].

3.9 2D-HSQC NMR of isolated lignin

The HSQC NMR spectra of isolated lignin provide more detailed information on the lignin structural moieties. Fig. S4 represents the 2D-HSQC NMR spectra of isolated lignin after NADES-ChCl/TA pretreatment. The spectral region can be seen in isolated lignin 2D-HSQC NMR spectra as aliphatic side chain region (δ_C/δ_H 50.00–90.00/2.40–5.70 ppm) and aromatic region (δ_C/δ_H 90.00–135.00/6.00–8.50 ppm), respectively [81]. The cross signals in 2D HSQC spectra are due to various structural moieties present in the isolated lignin; for instance, the aromatic regions in 2D HSQC spectra include cross signals originating from syringyl (S), guaiacyl (G), and p-hydroxyphenyl (H) units (Fig. 9). The assignment for the 2D-HSQC resonance signals is presented in Table 3. The characterized substructures and units of lignin are depicted in Fig. 10.

The side chain region of 2D-HSQC NMR spectra offers valuable information on the interunit linkages present in

Table 3 Assignments of main ^{13}C-^1H correlation peaks in 2D HSQC spectra of the isolated lignin

Label	δ_C/δ_H (ppm)	Assignment
B_β	53.04/3.52	C_β-H_β in phenylcoumaran β-5′ substructures (**B**)
C_β	53.10/3.12	C_β-H_β in resinol β-β′ substructures (**C**)
$-OCH_3$	55.52/3.82	C-H in methoxy groups
B_γ	66.85.3.40	C_γ-H_γ in phenylcoumaran β-5′ substructures (**B**)
$(A, A′)_\alpha$	71.97/4.27	C_α-H_α in β-O-4 substructures (**A** and **A′**)
C_γ	73.13/4.11	C_γ-H_γ in resinol β-β′ substructures (**C**)
$S_{2,6}$	106.84/7.21	$C_{2,6}$-$H_{2,6}$ in S units (**S**)
G_2	110.57/7.39	C_2-H_2 in guaiacyl units (**G**)
G_5	110.96/7.44	C_5-H_5 in guaiacyl units (**G**)
FA_2	111.03/7.28	C_2-H_2 in ferulate (**FA**)
G_6	112.57/7.44	C_6-H_6 in guaiacyl units (**G**)
FE_2	115.52/6.35	C_2-H_2 in ferulic ester (**FE**)
pCE_β	115.75/6.95	C_β-H_β in p-coumaroylated substructures (**A**)
FE_8	115.52/6.35	C_8-H_8 in ferulic ester (**FE**)
FE_6	122.77/7.08	C_6-H_6 in ferulic ester (**FE**)
FA_6	123.35/7.51	C_6-H_6 in ferulate (**FA**)
$H_{2,6}$	126.06/7.42	$C_{2,6}$-$H_{2,6}$ in p-hydroxyphenyl units (**H**)
$PCA_{2,6}$	130.03/7.51	C_2-H_2 and C_6-H_6 in p-coumarate (**PCA**)
$pCE_{2/6}$	131.50/7.80	$C_{2,6}$-$H_{2,6}$ in p-coumaroylated substructures
pCE_α	144.33/7.52	C_α-H_α in p-coumaroylated substructures

lignin (Fig. S5). The correlation signals from methoxy groups are more noticeable, with a signal at δ_C/δ_H 55.52/3.82 in the side chain region. The C_α-H_α correlation signals of β-O-4′ linkage of A and A′ substructures are observed at δ_C/δ_H 71.97/4.27 ppm. The C_β-H_β correlation signals in phenylcoumaran (β-5′) substructure B are observed at δ_C/δ_H 53.04/3.52 ppm and the C_γ-H_γ correlation signals at δ_C/δ_H 66.85/3.40 ppm. The correlating signals for resinol (β-β′)

Fig. 9 The aromatic regions in the 2D HSQC NMR spectra of isolated lignin
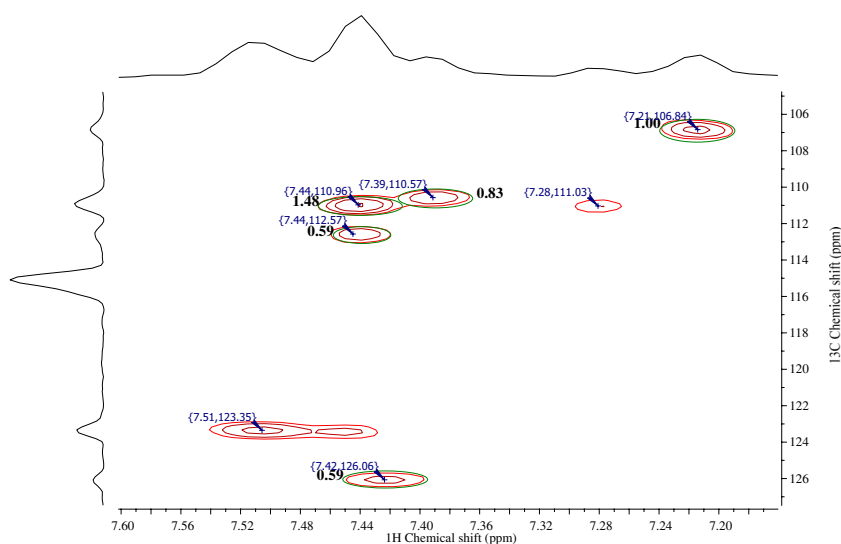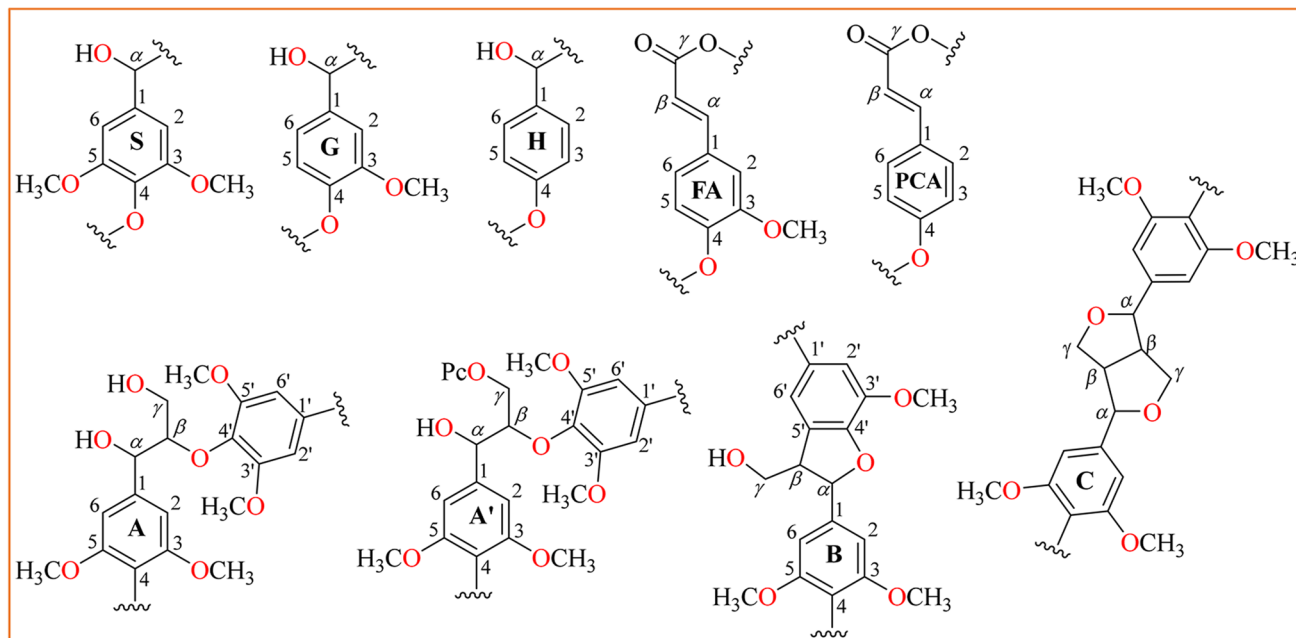
Fig. 10 Main lignin structures identified in the isolated lignin: S, syringyl unit; G, guaiacyl unit; H, *p*-hydroxyphenyl unit; FA, ferulic acid; PCA, *p*-coumaric acid; A and A′, γ-OH and γ-*p*-coumaroylated (Pc) β-O-4′; B, phenylcoumarane substructures formed by β-5′ and α-O-4′ linkages; C, resinol structures formed by β-β′/α-O-γ′/γ-O-α′ linkages

substructure C are observed with their C_β-H_β and C_γ-H_γ at δ_C/δ_H 53.10/3.12 and δ_C/δ_H 73.13/4.11, respectively. In the NADES-ChCl/TA isolated lignin, the prominent signal at δ_C/δ_H 106.84/7.21 ppm is linked with $C_{2,6}$-$H_{2,6}$ correlation in S units as depicted in Fig. 10. The isolated lignin aromatic moiety with G units' C_2-H_2, C_5-H_5, and C_6-H_6 correlation signals is observed at δ_C/δ_H 110.57/7.39, δ_C/δ_H 110.96/7.44, and δ_C/δ_H 112.57/7.44 ppm, respectively. The

correlation signals for $C_{2,6}$-$H_{2,6}$ in H units are observed at δ_C/δ_H 117.91/7.18 ppm. Also, other signals are observed in the aromatic regions such as correlation signals belonging to *p*-coumaric acid (PBA), ferulic acid (FA), ferulic esters, and *p*-coumaroylated substructures (Table 3). The correlation signals at δ_C/δ_H 130.03/7.51 are linked to C_2-H_2 and C_6-H_6 correlations in PCA. The area under the integration of the aromatic correlation signals provides insight
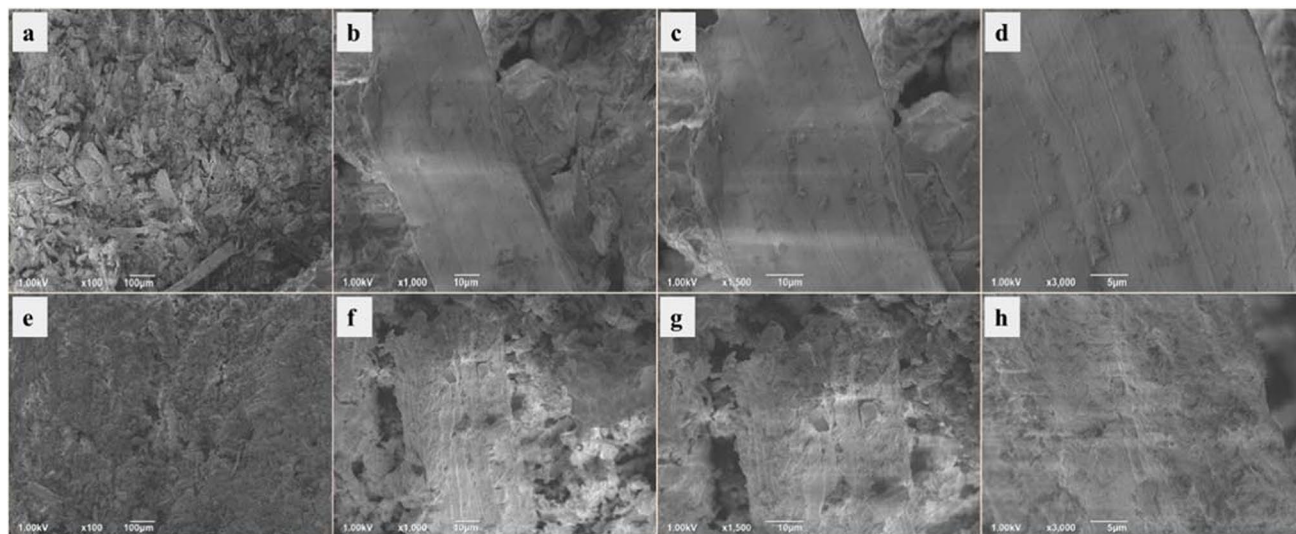

Fig. 11 SEM images of **a–d** untreated rice straw and **e–h** NADES-ChCl/TA pretreated rice straw

into the proportions of the S, G, and H units of lignin [81]. The current study indicates an S/G/H ratio of 1/2.9/0.59 for NADES-ChCl/TA isolated lignin from rice straw biomass.

3.10 SEM analysis

The surface morphology of pretreated and untreated rice straw was examined by SEM. Figure 11 represents the SEM images of raw and pretreated rice straw biomass at different magnifications. The surface was found to be more disrupted with increased coarseness following the NADES-ChCl/TA pretreatment. Thus, NADES-ChCl/TA was found to be more efficient in the generation of more pores and enhancing the surface area of rice straw biomass which is more beneficial for further downstream processes. The increase in surface area can be associated with the removal of hemicellulose and lignin [82].

3.11 ATR-FTIR characterization of pretreated rice straw

The structural differences between untreated and NADES-ChCl/TA-treated rice straw biomass were assessed by ATR-FTIR spectra for the optimized run as shown in Fig. 12. The broad band around 3310 cm^{-1} is due to O–H stretching vibration [83]. Absorption peaks at 2917 cm^{-1} are created primarily by the stretching vibration of C-H and are attributed to the cellulose crystalline structure in both untreated and pretreated samples [84]. The band at 1634 cm^{-1} and 1513 cm^{-1} is due to the aromatic skeleton and C=O stretching vibration associated with hemicellulose and lignin [82]. The absorption band at 1437 cm^{-1} and 1360 cm^{-1} is attributed to the C-H bending vibration of cellulosic main chains; these bands are stronger in pretreated samples which

Table 4 Change in crystallinity index of cellulose determined by ATR-FTIR and XRD analysis

Samples	HBI	TCI	LOI	CrI (%)
Untreated rice straw	0.9919	1.0045	1.0019	~67
NADES-ChCl/TA pre-treated rice straw	1.0057	1.0239	1.0036	~80

represents the crystalline band [84]. The band in the region of 950–1200 cm^{-1} with a common peak around 1055 cm^{-1} relates to the C-O and C–O–C stretching vibration of cellulose. The strong peak in NADES-ChCl/TA pretreated rice straw biomass also implies the exposure of more cellulose after pretreatment. The peak at around 830 cm^{-1} stronger in treated samples than untreated is indicative of β-1,4-glycosidic bond vibrations [85]. Additionally, cellulose crystallinity before and after pretreatment was assessed using HBI, TCI, LOI, and CrI (Table 4). The HBI, TCI, and LOI values of untreated (0.9919, 1.0045, and 1.0019) and pretreated rice straw biomass (1.0057, 1.0239, and 1.0036) are found to be increased after NADES-ChCl/TA pretreatment. These increased crystallinity indexes could be due to exposure to more crystalline cellulosic parts of the rice straw biomass following NADES-ChCl pretreatment [86]. A similar observation with a change in cellulose crystallinity (HBI, TCI, and LOI) was investigated by Gundupalli et al. during Napier grass pretreatment using pure mixed and diluted DES [38]. The HBI, TCI, and LOI of untreated Napier grass were found to be 0.95, 1.03, and 1.01, and that for mixed DES, pretreated Napier grass was 0.96, 1.02, and 1.02. Likewise, an investigation by Boonsombuti et al. using FTIR on the cellulose crystallinity of rice straw during ionic liquid, alkaline, and acid pretreatment also revealed an increased trend
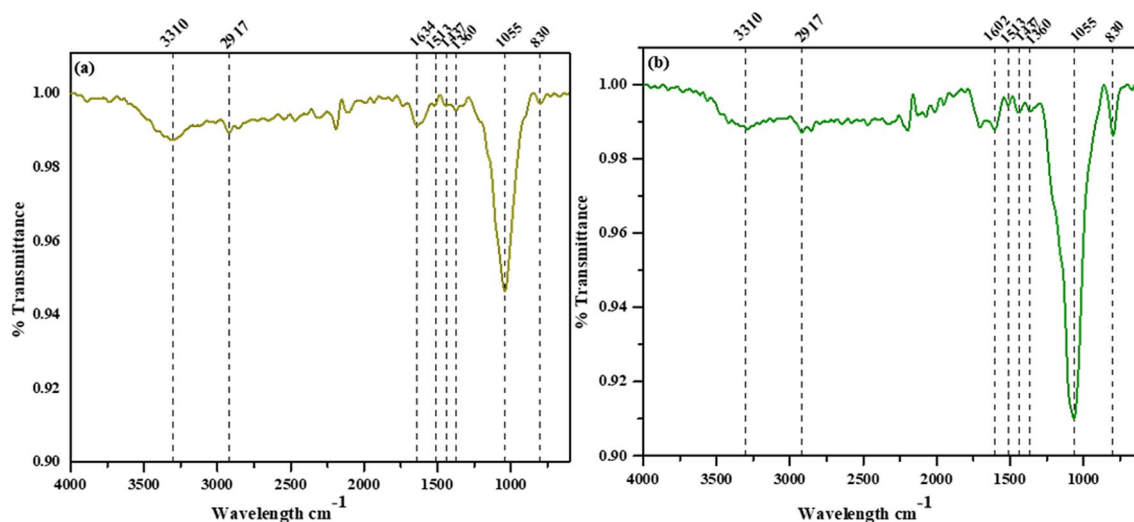

Fig. 12 ATR-FTIR characterization of **a** untreated rice straw and **b** pretreated rice straw

after pretreatment [83]. The FTIR crystallinity index during ionic liquid pretreatment in this study increased from 1.05 for untreated to 1.10 for ionic liquid pretreated rice straw biomass. Here, they concluded that this trend could be due to the elimination of hemicellulose and lignin during pretreatment. Therefore, the comparison of ATR-FTIR spectra of untreated and pretreated rice straw biomass in the current study also reveals an effective removal of lignin and hemicellulose components resulting in the production of CEM following the pretreatment of rice straw with NADES-ChCl/TA. The crystallinity of the untreated and NADES-ChCl/TA pretreated samples was subsequently investigated using XRD analysis.

3.12 XRD analysis

The XRD pattern of the NADES-ChCl/TA pretreated rice straw sample was compared to that of untreated rice straw as shown in Fig. 11. The crystallinity index (CrI), which corresponds to the cellulose I polymorph at 2θ ~22° and ~18°, was substantially higher in the pretreated rice straw than in the untreated [87]. The CrI of untreated rice straw biomass (~67%) was increased after pretreatment (~80%) as represented in Fig. 13 (Table 4). The increase in CrI was because of the removal of amorphous hemicellulose and lignin through NADES-ChCl/TA pretreatment [42]. At optimal conditions, the pretreatment temperature also has a strong ability to partially break up and reduce the amorphous regions of rice straw biomass, which exposes more crystalline cellulose and gives a higher degree of crystallinity. A similar observation with an increase in CrI of pretreated rice straw was also observed in a report by Freitas et al. after alkaline pretreatment [88]. Also, during DES pretreatment of rice straw, Hou et al. found an increase in CrI for pretreated biomass, which they attributed to the removal of hemicellulose and lignin content in the pretreated rice straw than that

of the untreated [18]. Similarly, an investigation of different combinatorial pretreatment techniques utilizing DES solvent to rice straw by Sawhney et al. found the CrI of rice straw increased from 57.18 to 59–61% [42]. In agreement with the current investigation, the DES pretreatment of various LCBs can be correlated. For instance, Wang et al. reported pretreatment of hybrid *Pennisetum* biomass with ChCl/glycerol (ChCl/G) combined with different Lewis acids significantly boosted the biomass CrI (59.60–70.80%) over that of native biomass (58.14%) [89]. In another study by Shen et al., it was observed that the ChCl/lactic acid pretreatment enhanced the CrI of *Eucalyptus camaldulensis* LCB from 50.4 to 68.3% [90]. The increase in the CrI indicates a rise in the cellulose fraction in the biomass rather than an increase in the cellulose content [83]. Thus, DES pretreatment breaks up the highly ordered raw LCB and gets rid of some of its amorphous parts, which makes it easier for enzymes to digest.

3.13 DES recovery and recycle

To develop an economically effective biorefinery, the recyclability of the DES is of key importance. The ability to recycle green solvents is another important problem that needs to be addressed. In this context, the recyclability of NADES-ChCl/TA was investigated in the optimized pretreatment condition. The extra water from the liquid hydrolysate following lignin isolation was evaporated under reduced vapor pressure until the weight remained constant and the viscous liquid phase appeared. The recovered NADES-ChCl/TA was used in the pretreatment under optimized conditions (117 °C; 137.96 min; NADES-ChCl/TA concentration 27.71%, 10% biomass loading). The recycling of NADES-ChCl/TA was repeated 7 times. The NADES-ChCl/TA regenerated were characterized with ATR-FTIR and spectra compared to the
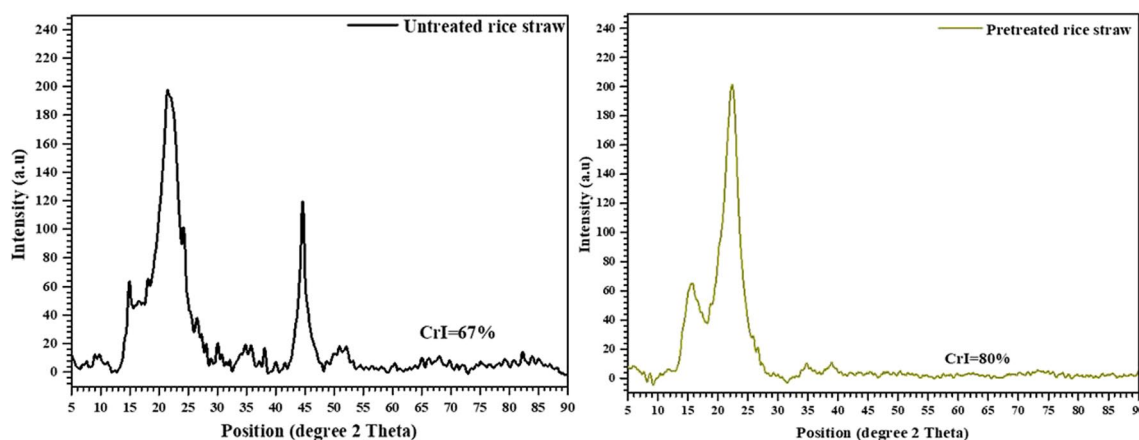

Fig. 13 Comparison of X-ray diffraction patterns for rice straw biomass untreated and pretreated with NADES-ChCl/TA

Fig. 14 DES recyclability studies with liquid hydrolysate profile
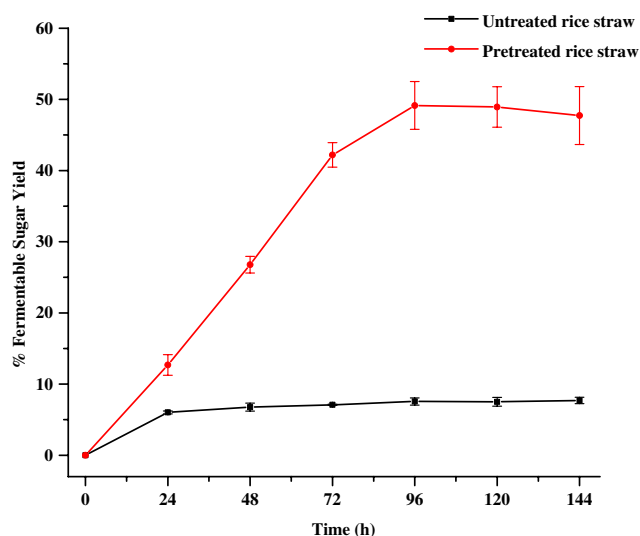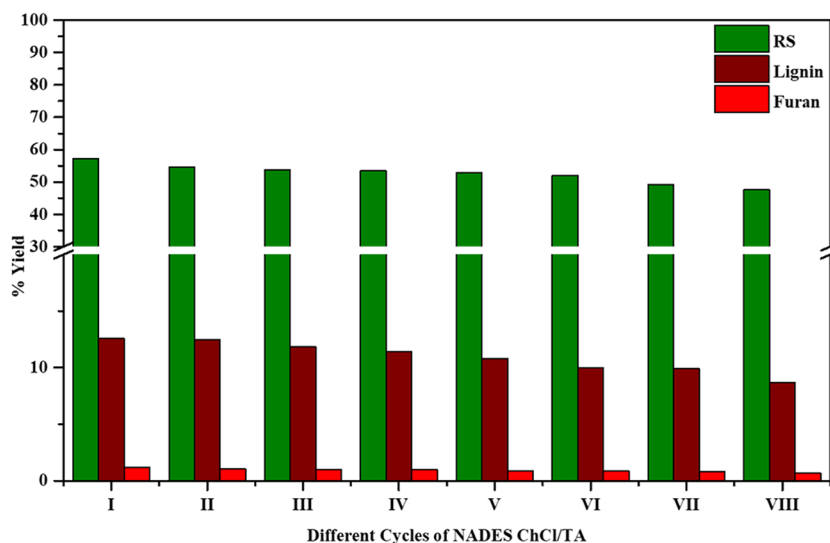

Fig. 15 Saccharification study of NADES-ChCl/TA pretreated and untreated rice straw samples

native one. The similarity in the ATR-FTIR spectra indicates that the functional groups in the raw NADES-ChCl/TA were preserved in the NADES-ChCl/TA obtained after eight cycles (Fig. S3). The efficiencies of DES-ChCl/TA in each cycle can be observed with the liquid hydrolysate profile in each cycle as shown in Fig. 14. The RS percentage varies from around 56 to 48% whereas lignin and furan compounds vary from 12.6 to 8.7% and 1.2 to 0.7% from first to eighth cycle. This nominal decrease of three responses from the first to the eighth cycle shows a high level of recyclability. The increase in contaminants in the DES after each recycling could be the reason for the reduction in DES pretreatment effectiveness. It has been observed that there are carboxylic acids produced

by the degradation of cellulose and hemicellulose as well as phenolic compounds produced by the dissolution of lignin leading to decreased pretreatment effectiveness of NADES-ChCl/TA [91]. The findings of this study show that NADES-ChCl/TA is renewable and can be recycled and reused in biomass pretreatment. Thus, NADES-ChCl/TA has the potential to lower the cost and chemical uses for effective LCB pretreatment.

3.14 Enzymatic hydrolysis

The effect of NADES-ChCl/TA pretreatment on the production of fermentable sugar from rice straw observed using commercial enzymes cellulase and β-glucosidase is shown in Fig. 15. Comparisons of raw and NADES-pretreated rice straw in terms of fermentable sugar production were evaluated. It can be seen in Fig. 15 that after 24 h of enzymatic hydrolysis, NADES-ChCl/TA-treated rice straw produced 12.68% of RS, which was substantially more than the yield obtained in the same amount of time through hydrolysis from untreated biomass (~6.14% of RS). Similarly, there is an increase in the production of fermentable sugar till 96 h for pretreated rice straw, whereas a negligible increase was observed for untreated rice straw hydrolysis during similar time intervals. The maximum RS of 49.15% was observed at the interval of 96 h from pretreated rice which is 6.5 times higher than the fermentable sugar produced via enzymatic hydrolysis of untreated rice straw (~7.47% of RS) (Fig. 15). The observation was based on the total cellulose and hemicellulose components available in the untreated rice straw biomass. This increase in the RS recovery from NADES-ChCl/TA pretreated sample is due to high lignin removal and carbohydrate recovery. The lignin in untreated rice straw may inhibit the saccharification
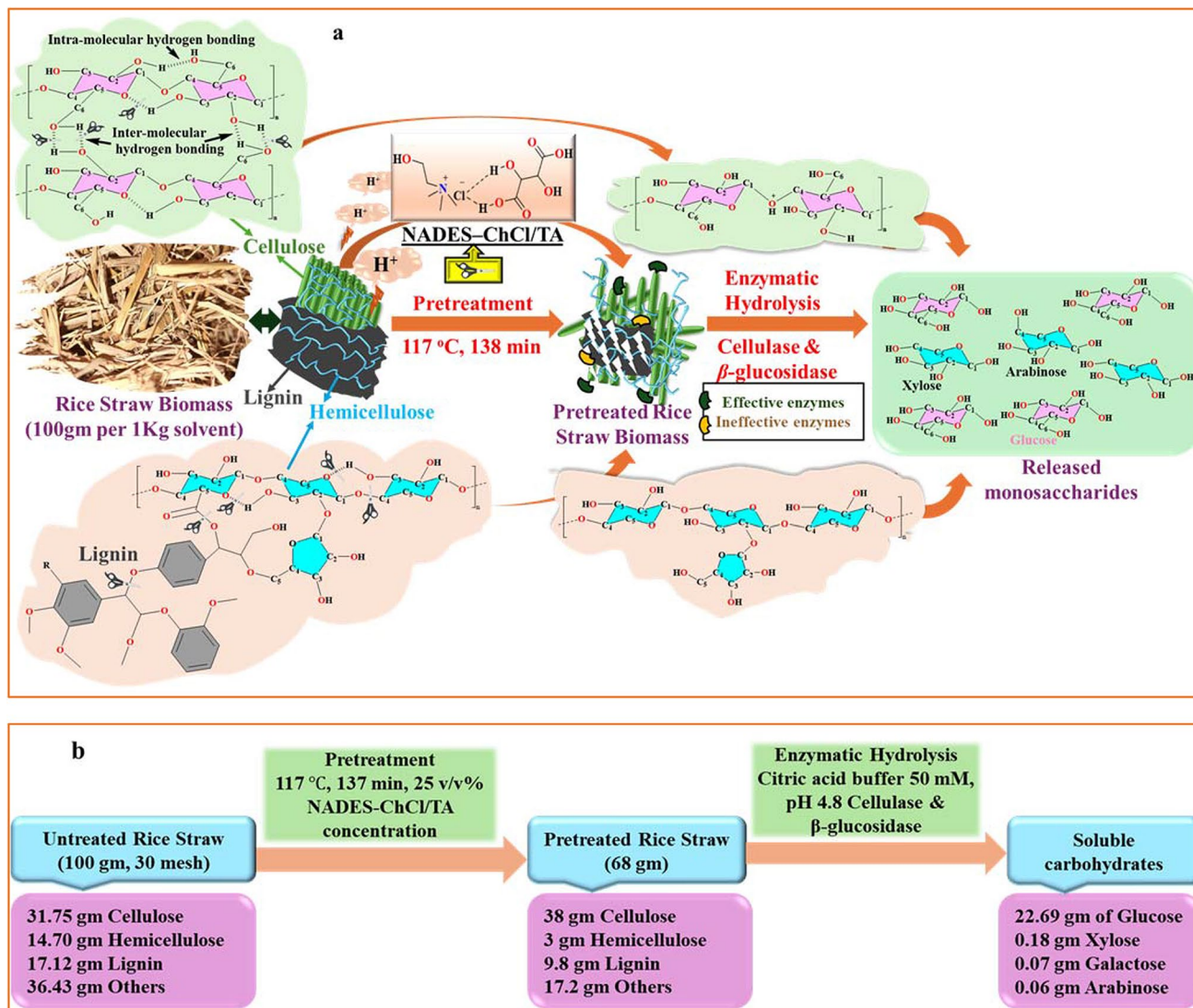
Fig. 16 **a** Mechanism of NADES-ChCl/TA pretreatment rice straw biomass and enzymatic hydrolysis. **b** Mass balance of NADES-ChCl/TA pretreatment of rice straw biomass

process by adsorbing cellulase enzymes, whereas the residual lignin in treated samples has low enzyme adsorption [92]. The observation at the 120-h sample gave the RS yield slightly lower than that of 96 h. Also, there has been more decrease in RS yield at 144 h for NADES-ChCl/TA pretreated rice straw samples with constant release of RS from raw sample hydrolysis. This decrease is due to an increase in the saturation for RS production

with time intervals. Thus, there were significant correlations between pretreatment temperature and DES concentration sugar yield from enzymatic hydrolysis. The NADES-ChCl/TA pretreatment gave a high recovery of fermentable sugar with more effective enzymatic hydrolysis at around the 96th hour which may be due to higher delignification of biomass with a significant effect of the process variables at optimized conditions.

Table 5 Compositional analysis of rice straw for determination of delignification and hemicellulose removal

Sample	Cellulose (%)	Hemicellulose (%)	Lignin (%)	Delignification (%)	Hemicellulose removal (%)
Untreated	31.75 ± 3.09	14.70 ± 1.07	17.12 ± 0.65	-	-
NADES-ChCl/ TA pretreated	52.35 ± 2.49	3.90 ± 0.83	13.98 ± 1.56	18.34	73.46

3.15 Mechanism of NADES-ChCl/TA pretreatment of rice straw

The possible structural transformation of the major constituents during NADES-ChCl/TA pretreatment of rice straw is presented in Fig. 16a. The action of NADES-ChCl/TA on rice straw during pretreatment breaks the complex structure of rice straw biomass. The various kinds of bonding, including hydrogen bonds and van der Waal forces, found in the molecular structures of cellulose and hemicellulose are weakened by NADES-ChCl/TA's interaction with these materials in LCB [93]. The chloride anion in NADES-ChCl/TA establishes effective hydrogen bonding interaction with hydroxyl groups and carboxyl groups of lignin, disrupting the intramolecular hydrogen bonds between lignin units [14]. Also, the NADES-ChCl/TA due to its TA as HBD is slightly acidic. The NADES-ChCl/TA offers the removal of hemicellulose (73.46%) and delignification (18.34%) breaking the complex structure of rice straw biomass (Table 5). After NADES-ChCl/TA pretreatment, the cell wall of rice straw underwent modification, including a reduction in lignin surface, an increased porosity, and a rougher surface, which will result in greater enzymatic accessibility.

The process mass balance was revealed as presented in Fig. 16b; it involves NADES-ChCl/TA pretreatment and enzymatic hydrolysis of rice straw biomass. The calculation in Fig. 16b was based on the 100 g of untreated rice straw biomass. Once 100 g of rice straw (31.75 g cellulose, 14.70 g hemicellulose, 17.12 g lignin) was subjected to pretreatment at optimal condition (117 °C, 137 min, 25 v/v% NADES-ChCl/TA concentration at 10% solid loading), ~68 g of the pretreated rice straw was left as a solid residue. The pretreated rice straw was composed of 38 g cellulose, 3 g hemicellulose, and 9.8 g lignin. A good amount of hemicellulose and lignin removal has occurred with the retention of cellulosic material in the pretreated rice straw biomass. The process of enzymatic hydrolysis facilitated the release of glucose from cellulose, while the enzymatic attack on hemicellulose revealed the presence of xylose. The NADES-ChCl/TA pretreated rice straw was enzymatically hydrolyzed using cellulase and β-glucosidase in citric acid buffer solution (pH 4.8, 50 mM) to produce 25 g of glucose, 0.19 g xylose, 0.14 g galactose, and 0.06 g arabinose. Thus, the results indicate that the NADES-ChCl pretreatment of rice straw biomass can be done under mild conditions to improve the degradability of rice straw biomass.

4 Conclusion

In summary, this study showed a green approach to the pretreatment of rice straw biomass, an agricultural residue for value-added product recovery using natural DES. The effect of different concentrations of NADES-ChCl/TA was investigated with various levels of temperature and pretreatment time. The optimum pretreatment conditions were observed to be 117.63 °C, 137.96 min, and 25.01 v/v% NADES-ChCl/TA concentration. The pretreatment at optimal conditions resulted in $57.11 \pm 1.43\%$ RS and 12.58 ± 0.23 lignin recovery. A lignin yield of 45 ± 2.02 mg per gram was isolated from rice straw under optimal conditions. The result obtained from ATR-FTIR spectra shows efficient lignin removal and was also found to be consistent with XRD analysis. The present study demonstrates the feasibility of using natural green solvents for a more sustainable biorefinery.

Declarations

References

1. Velvizhi G, Balakumar K, Shetti NP et al (2022) Integrated biorefinery processes for conversion of lignocellulosic biomass to value added materials: paving a path towards circular economy. Bioresour Technol 343:126151. https://doi.org/10.1016/j.biortech.2021.126151

2. Takada M, Chandra R, Wu J, Saddler JN (2020) The influence of lignin on the effectiveness of using a chemithermomechanical pulping based process to pretreat softwood chips and pellets prior to enzymatic hydrolysis. Bioresour Technol 302:122895. https://doi.org/10.1016/j.biortech.2020.122895

3. Florindo C, Oliveira MM, Branco LC, Marrucho IM (2017) Carbohydrates-based deep eutectic solvents: thermophysical properties and rice straw dissolution. J Mol Liq 247:441–447. https://doi.org/10.1016/j.molliq.2017.09.026

4. Isikgor FH, Becer CR (2015) Lignocellulosic biomass: a sustainable platform for the production of bio-based chemicals and polymers. Polym Chem 6:4497–4559. https://doi.org/10.1039/c5py00263j

5. Cheng YS, Mutrakulcharoen P, Chuetor S et al (2020) Recent situation and progress in biorefining process of lignocellulosic biomass: toward green economy. Appl Sci Eng Prog 13:299–311. https://doi.org/10.14416/J.ASEP.2020.08.002

6. Sriariyanun M, Gundupalli MP, Phakeenuya V et al (2024) Biorefinery approaches for production of cellulosic ethanol fuel using recombinant engineered microorganisms. J Appl Sci Eng 27:1985–2005. https://doi.org/10.6180/jase.202402_27(2).0001

7. Etale A, Onyianta AJ, Turner SR, Eichhorn SJ (2023) Cellulose: a review of water interactions, applications in composites, and water treatment. Chem Rev 123:2016–2048. https://doi.org/10.1021/acs.chemrev.2c00477

8. Agbor VB, Cicek N, Sparling R et al (2011) Biomass pretreatment: fundamentals toward application. Biotechnol Adv 29:675–685. https://doi.org/10.1016/j.biotechadv.2011.05.005

9. Aung EM, Endo T, Fujii S et al (2018) Efficient pretreatment of bagasse at high loading in an ionic liquid. Ind Crops Prod 119:243–248. https://doi.org/10.1016/j.indcrop.2018.04.006

10. Gundupalli MP, Bano K, Panda TK et al (2022) Understanding the effect of low-concentrated protic ionic liquids (PILs) on coconut (Cocos nucifera) residues. Biomass Convers Biorefinery. https://doi.org/10.1007/s13399-022-02572-4

11. An YX, Zong MH, Wu H, Li N (2015) Pretreatment of lignocellulosic biomass with renewable cholinium ionic liquids: biomass fractionation, enzymatic digestion and ionic liquid reuse. Bioresour Technol 192:165–171. https://doi.org/10.1016/j.biortech.2015.05.064

12. Hou XD, Li N, Zong MH (2013) Significantly enhancing enzymatic hydrolysis of rice straw after pretreatment using renewable ionic liquid-water mixtures. Bioresour Technol 136:469–474. https://doi.org/10.1016/j.biortech.2013.02.118

13. Zhang M, Tian R, Tang S et al (2023) Multistage treatment of bamboo powder waste biomass: highly efficient and selective isolation of lignin components. Waste Manag 166:35–45. https://doi.org/10.1016/j.wasman.2023.04.040

14. Wu M, Di J, Gong L et al (2023) Enhanced adipic acid production from sugarcane bagasse by a rapid room temperature pretreatment. Chem Eng J 452:139320. https://doi.org/10.1016/j.cej.2022.139320

15. Tang Z, Wu C, Tang W et al (2023) A novel cetyltrimethylammonium bromide-based deep eutectic solvent pretreatment of rice husk to efficiently enhance its enzymatic hydrolysis. Bioresour Technol 376:128806. https://doi.org/10.1016/j.biortech.2023.128806

16. Chen Y, Yang D, Tang W et al (2023) Improved enzymatic saccharification of bulrush via an efficient combination pretreatment. Bioresour Technol 385:129369. https://doi.org/10.1016/j.biortech.2023.129369

17. Tang Z, Yang D, Tang W et al (2023) Combined sulfuric acid and choline chloride/glycerol pretreatment for efficiently enhancing enzymatic saccharification of reed stalk. Bioresour Technol 387:129554. https://doi.org/10.1016/j.biortech.2023.129554

18. Hou XD, Feng GJ, Ye M et al (2017) Significantly enhanced enzymatic hydrolysis of rice straw via a high-performance two-stage deep eutectic solvents synergistic pretreatment. Bioresour Technol 238:139–146. https://doi.org/10.1016/j.biortech.2017.04.027

19. Xing W, Xu G, Dong J et al (2018) Novel dihydrogen-bonding deep eutectic solvents: pretreatment of rice straw for butanol fermentation featuring enzyme recycling and high solvent yield. Chem Eng J 333:712–720. https://doi.org/10.1016/j.cej.2017.09.176

20. Zulkefli S, Abdulmalek E, Abdul Rahman MB (2017) Pretreatment of oil palm trunk in deep eutectic solvent and optimization of enzymatic hydrolysis of pretreated oil palm trunk. Renew Energy 107:36–41. https://doi.org/10.1016/j.renene.2017.01.037

21. Okur M, Eslek Koyuncu DD (2020) Investigation of pretreatment parameters in the delignification of paddy husks with deep eutectic solvents. Biomass Bioenerg 142:105811. https://doi.org/10.1016/j.biombioe.2020.105811

22. Alvarez-Vasco C, Ma R, Quintero M et al (2016) Unique low-molecular-weight lignin with high purity extracted from wood by deep eutectic solvents (DES): a source of lignin for valorization. Green Chem 18:5133–5141. https://doi.org/10.1039/c6gc01007e

23. Chen Z, Ragauskas A, Wan C (2020) Lignin extraction and upgrading using deep eutectic solvents. Ind Crops Prod 147:112241. https://doi.org/10.1016/j.indcrop.2020.112241

24. Dai Y, van Spronsen J, Witkamp GJ et al (2013) Natural deep eutectic solvents as new potential media for green technology. Anal Chim Acta 766:61–68. https://doi.org/10.1016/j.aca.2012.12.019

25. Kumar AK, Parikh BS, Pravakar M (2016) Natural deep eutectic solvent mediated pretreatment of rice straw: bioanalytical characterization of lignin extract and enzymatic hydrolysis of pretreated biomass residue. Environ Sci Pollut Res 23:9265–9275. https://doi.org/10.1007/s11356-015-4780-4

26. Xu H, Peng J, Kong Y et al (2020) Key process parameters for deep eutectic solvents pretreatment of lignocellulosic biomass materials: a review. Bioresour Technol 310:123416. https://doi.org/10.1016/j.biortech.2020.123416

27. Scelsi E, Angelini A, Pastore C (2021) Deep eutectic solvents for the valorisation of lignocellulosic biomasses towards fine chemicals. Biomass 1:29–59. https://doi.org/10.3390/biomass1010003

28. Jose D, Tawai A, Divakaran D et al (2023) Integration of deep eutectic solvent in biorefining process of lignocellulosic biomass valorization. Bioresour Technol Reports 21:101365. https://doi.org/10.1016/j.biteb.2023.101365

29. Li P, Yang C, Jiang Z et al (2023) Lignocellulose pretreatment by deep eutectic solvents and related technologies: a review. J Bioresour Bioprod 8:33–44. https://doi.org/10.1016/j.jobab.2022.11.004

30. Xu H, Kong Y, Peng J et al (2021) Mechanism of deep eutectic solvent delignification: insights from molecular dynamics simulations. ACS Sustain Chem Eng 9:7101–7111. https://doi.org/10.1021/acssuschemeng.1c01260

31. Panakkal EJ, Cheenkachorn K, Chuetor S, et al (2022) Optimization of deep eutectic solvent pretreatment for bioethanol production from Napier grass. Sustain Energy Technol Assessments 54:102856. https://doi.org/10.1016/j.seta.2022.102856

32. Comuzzo P, Battistutta F (2018) Acidification and pH control in red wines. In: Red wine technology, Academic Press. Elsevier Inc, pp 17–34

33. Tang Z, Wu C, Tang W et al (2023) Enhancing enzymatic saccharification of sunflower straw through optimal tartaric acid hydrothermal pretreatment. Bioresour Technol 385:129279. https://doi.org/10.1016/j.biortech.2023.129279

34. Gabriele F, Chiarini M, Germani R et al (2019) Effect of water addition on choline chloride/glycol deep eutectic solvents: characterization of their structural and physicochemical properties. J Mol Liq 291:111301. https://doi.org/10.1016/j.molliq.2019.111301

35. Sunar SL, Oruganti RK, Bhattacharyya D et al (2024) Pretreatment of sugarcane bagasse using ionic liquid for enhanced enzymatic saccharification and lignin recovery: process optimization by response surface methodology. Cellulose. https://doi.org/10.1007/s10570-024-05768-1

36. Sluiter A, Hames B, Ruiz R et al (2008) Determination of structural carbohydrates and lignin in biomass. Lab Anal Proced 1617:1–16

37. Maibam PD, Goyal A (2022) Approach to an efficient pretreatment method for rice straw by deep eutectic solvent for high saccharification efficiency. Bioresour Technol 351:127057. https://doi.org/10.1016/j.biortech.2022.127057

38. Gundupalli MP, Cheenkachorn K, Chuetor S et al (2023) Assessment of pure, mixed and diluted deep eutectic solvents on Napier grass (Cenchrus purpureus): compositional and characterization studies of cellulose, hemicellulose and lignin. Carbohydr Polym 306:120599. https://doi.org/10.1016/j.carbpol.2023.120599

39. Kruer-Zerhusen N, Cantero-Tubilla B, Wilson DB (2018) Characterization of cellulose crystallinity after enzymatic treatment using Fourier transform infrared spectroscopy (FTIR). Cellulose 25:37–48. https://doi.org/10.1007/s10570-017-1542-0

40. Vaid S, Sharma S, Dutt HC et al (2021) One pot consolidated bioprocess for conversion of Saccharum spontaneum biomass to ethanol-biofuel. Energy Convers Manag 250:114880. https://doi.org/10.1016/j.enconman.2021.114880

41. French AD (2014) Idealized powder diffraction patterns for cellulose polymorphs. Cellulose 21:885–896. https://doi.org/10.1007/s10570-013-0030-4

42. Sawhney D, Vaid S, Bangotra R et al (2023) Proficient bioconversion of rice straw biomass to bioethanol using a novel combinatorial pretreatment approach based on deep eutectic solvent, microwave irradiation and laccase. Bioresour Technol 375:128791. https://doi.org/10.1016/j.biortech.2023.128791

43. Sorn V, Chang KL, Phitsuwan P et al (2019) Effect of microwave-assisted ionic liquid/acidic ionic liquid pretreatment on the morphology, structure, and enhanced delignification of rice straw. Bioresour Technol 293:121929. https://doi.org/10.1016/j.biortech.2019.121929

44. Singh A, Bishnoi NR (2012) Optimization of enzymatic hydrolysis of pretreated rice straw and ethanol production. Appl Microbiol Biotechnol 93:1785–1793. https://doi.org/10.1007/s00253-012-3870-1

45. Kumar V, Patel SKS, Gupta RK, et al (2019) Enhanced saccharification and fermentation of rice straw by reducing the concentration of phenolic compounds using an immobilized enzyme cocktail. Biotechnol J 14:1800468. https://doi.org/10.1002/biot.201800468

46. Gummert M, Van Hung N, Chivenge P, Douthwaite B (2019) Sustainable rice straw management. Sustain Rice Straw Manag 1–192. https://doi.org/10.1007/978-3-030-32373-8

47. Vieira L, Schennach R, Gollas B (2015) In situ PM-IRRAS of a glassy carbon electrode/deep eutectic solvent interface. Phys Chem Chem Phys 17:12870–12880. https://doi.org/10.1039/c5cp00070j

48. Liang X, Fu Y, Chang J (2019) Effective separation, recovery and recycling of deep eutectic solvent after biomass fractionation with membrane-based methodology. Sep Purif Technol 210:409–416. https://doi.org/10.1016/j.seppur.2018.08.021

49. Othman ZS, Hassan NH, Zubairi SI (2015) Alcohol based-deep eutectic solvent (DES) as an alternative green additive to increase rotenone yield. AIP Conf Proc 1678:1–9. https://doi.org/10.1063/1.4931283

50. Khan N, Vijayan N, Shandilya K et al (2020) Single crystal growth of l-tartaric acid and its characterization for optical applications. J Mater Sci Mater Electron 31:4494–4502. https://doi.org/10.1007/s10854-020-02998-4

51. Koutsoukos S, Tsiaka T, Tzani A et al (2019) Choline chloride and tartaric acid, a natural deep eutectic solvent for the efficient extraction of phenolic and carotenoid compounds. J Clean Prod 241:118384. https://doi.org/10.1016/j.jclepro.2019.118384

52. Triki A, Dittmer J, Ben HM et al (2016) Spectroscopy analyses of hybrid unsaturated polyester composite reinforced by Alfa, wool, and thermo-binder fibres. Polym Sci - Ser A 58:255–264. https://doi.org/10.1134/S0965545X16020188

53. Zhu S, Li H, Zhu W et al (2016) Vibrational analysis and formation mechanism of typical deep eutectic solvents: an experimental and theoretical study. J Mol Graph Model 68:158–175. https://doi.org/10.1016/j.jmgm.2016.05.003

54. Sidik DAB, Ngadi N, Amin NAS (2013) Optimization of lignin production from empty fruit bunch via liquefaction with ionic liquid. Bioresour Technol 135:690–696. https://doi.org/10.1016/j.biortech.2012.09.041

55. Pan M, Zhao G, Ding C et al (2017) Physicochemical transformation of rice straw after pretreatment with a deep eutectic solvent of choline chloride/urea. Carbohydr Polym 176:307–314. https://doi.org/10.1016/j.carbpol.2017.08.088

56. Raj T, Gaur R, Dixit P et al (2016) Ionic liquid pretreatment of biomass for sugars production: driving factors with a plausible mechanism for higher enzymatic digestibility. Carbohydr Polym 149:369–381. https://doi.org/10.1016/j.carbpol.2016.04.129

57. Chen WH, Ye SC, Sheen HK (2012) Hydrolysis characteristics of sugarcane bagasse pretreated by dilute acid solution in a microwave irradiation environment. Appl Energy 93:237–244. https://doi.org/10.1016/j.apenergy.2011.12.014

58. Tsegaye B, Balomajumder C, Roy P (2020) Organosolv pretreatments of rice straw followed by microbial hydrolysis for efficient biofuel production. Renew Energy 148:923–934. https://doi.org/10.1016/j.renene.2019.10.176

59. Weerachanchai P, Leong SSJ, Chang MW et al (2012) Improvement of biomass properties by pretreatment with ionic liquids for bioconversion process. Bioresour Technol 111:453–459. https://doi.org/10.1016/j.biortech.2012.02.023

60. Li W, Sun N, Stoner B et al (2011) Rapid dissolution of lignocellulosic biomass in ionic liquids using temperatures above the glass transition of lignin. Green Chem 13:2038–2047. https://doi.org/10.1039/c1gc15522a

61. Poy H, Lladosa E, Gabaldón C, Loras S (2021) Optimization of rice straw pretreatment with 1-ethyl-3-methylimidazolium acetate by the response surface method. Biomass Convers Biorefinery. https://doi.org/10.1007/s13399-021-02111-7

62. Fendt S, Padmanabhan S, Blanch HW, Prausnitz JM (2011) Viscosities of acetate or chloride-based ionic liquids and some of their mixtures with water or other common solvents. J Chem Eng Data 56:31–34. https://doi.org/10.1021/je1007235

63. Saha K, Dasgupta J, Chakraborty S et al (2017) Optimization of lignin recovery from sugarcane bagasse using ionic liquid aided pretreatment. Cellulose 24:3191–3207. https://doi.org/10.1007/s10570-017-1330-x

64. Serna-Loaiza S, Dias M, Daza-Serna L et al (2022) Integral analysis of liquid-hot-water pretreatment of wheat straw: evaluation of the production of sugars, degradation products, and Lignin. Sustain 4:362. https://doi.org/10.3390/su14010362

65. Khamis NA, Shamsudin S, Abd Rahman NS, Kasim KF (2019) Effects of autohydrolysis on rice biomass for reducing sugars production. Mater Today Proc 16:2078–2087. https://doi.org/10.1016/j.matpr.2019.06.095

66. Agrawal R, Verma A, Singhania RR et al (2021) Current understanding of the inhibition factors and their mechanism of action for the lignocellulosic biomass hydrolysis. Bioresour Technol 332:125042. https://doi.org/10.1016/j.biortech.2021.125042

67. Guadix-Montero S, Sankar M (2018) Review on catalytic cleavage of C-C inter-unit linkages in lignin model compounds: towards lignin depolymerisation. Top Catal 61:183–198. https://doi.org/10.1007/s11244-018-0909-2

68. Zhang C, Shen X, Jin Y et al (2023) Catalytic strategies and mechanism analysis orbiting the center of critical intermediates in lignin depolymerization. Chem Rev 123:4510–4601. https://doi.org/10.1021/acs.chemrev.2c00664

69. Calvo-Flores FG, Dobado JA (2010) Lignin as renewable raw material. Chemsuschem 3:1227–1235. https://doi.org/10.1002/cssc.201000157

70. Qiu Y, Zhong D, Zeng K et al (2023) Evolution of lignin pyrolysis heavy components through the study of representative lignin monomers. Fuel Process Technol 250:107910. https://doi.org/10.1016/j.fuproc.2023.107910

71. Xu F, Sun J, Wehrs M et al (2018) Biocompatible choline-based deep eutectic solvents enable one-pot production of cellulosic

ethanol. ACS Sustain Chem Eng 6:8914–8919. https://doi.org/10.1021/acssuschemeng.8b01271

72. Guo Z, Zhang Q, You T et al (2019) Short-time deep eutectic solvent pretreatment for enhanced enzymatic saccharification and lignin valorization. Green Chem 21:3099–3108. https://doi.org/10.1039/c9gc00704k

73. Chen Y, Ma C, Tang W, He Y (2023) Bioresource technology comprehensive understanding of enzymatic saccharification of betaine : lactic acid-pretreated sugarcane bagasse. Bioresour Technol 386:129485. https://doi.org/10.1016/j.biortech.2023.129485

74. Shweta K, Jha H (2015) Rice husk extracted lignin-TEOS biocomposites: effects of acetylation and silane surface treatments for application in nickel removal. Biotechnol Reports 7:95–106. https://doi.org/10.1016/j.btre.2015.05.003

75. Shen D, Liu G, Zhao J et al (2015) Thermo-chemical conversion of lignin to aromatic compounds: effect of lignin source and reaction temperature. J Anal Appl Pyrolysis 112:56–65. https://doi.org/10.1016/j.jaap.2015.02.022

76. Ghaffar SH, Fan M (2014) Lignin in straw and its applications as an adhesive. Int J Adhes Adhes 48:92–101. https://doi.org/10.1016/j.ijadhadh.2013.09.001

77. Akhramez S, Fatimi A, Okoro OV et al (2022) The circular economy paradigm: modification of bagasse-derived lignin as a precursor to sustainable hydrogel production. Sustain 14:8791. https://doi.org/10.3390/su14148791

78. Mahmood N, Yuan Z, Schmidt J, Xu C (2013) Production of polyols via direct hydrolysis of kraft lignin: effect of process parameters. Bioresour Technol 139:13–20. https://doi.org/10.1016/j.biortech.2013.03.199

79. Xue BL, Wen JL, Sun RC (2015) Producing lignin-based polyols through microwave-assisted liquefaction for rigid polyurethane foam production. Materials (Basel) 8:586–599. https://doi.org/10.3390/ma8020586

80. Rashid T, Kait CF, Regupathi I, Murugesan T (2016) Dissolution of kraft lignin using protic ionic liquids and characterization. Ind Crops Prod 84:284–293. https://doi.org/10.1016/j.indcrop.2016.02.017

81. Oruganti RK, Sunar SL, Panda TK et al (2023) Bioresource technology reports kraft lignin recovery from de-oiled Jatropha curcas seed by potassium hydroxide pretreatment and optimization using response surface methodology. Bioresour Technol Reports 23:101572. https://doi.org/10.1016/j.biteb.2023.101572

82. Kumari D, Singh R (2022) Rice straw structure changes following green pretreatment with petha wastewater for economically viable bioethanol production. Sci Rep 12:1–10. https://doi.org/10.1038/s41598-022-14627-7

83. Boonsombuti A, Trisinsub O, Luengnaruemitchai A (2020) Comparative study of three chemical pretreatments and their effects on the structural changes of rice straw and butanol production. Waste Biomass Valorization 11:2771–2781. https://doi.org/10.1007/s12649-019-00622-z

84. Hartati I, Sulistyo H, Sediawan WB et al (2021) Microwave-assisted urea-based-hydrotropic pretreatment of rice straw: experimental data and mechanistic kinetic models. ACS Omega 6:13225–13239. https://doi.org/10.1021/acsomega.1c01084

85. Atykyan N, Revin V, Shutova V (2020) Raman and FT-IR spectroscopy investigation the cellulose structural differences from bacteria Gluconacetobacter sucrofermentans during the different regimes of cultivation on a molasses media. AMB Express 10:84. https://doi.org/10.1186/s13568-020-01020-8

86. Ayeni AO, Daramola MO (2017) Lignocellulosic biomass waste beneficiation: evaluation of oxidative and non-oxidative pretreatment methodologies of South African corn cob. J Environ Chem Eng 5:1771–1779. https://doi.org/10.1016/j.jece.2017.03.019

87. Liu Y, Zheng X, Tao S et al (2021) Process optimization for deep eutectic solvent pretreatment and enzymatic hydrolysis of sugar cane bagasse for cellulosic ethanol fermentation. Renew Energy 177:259–267. https://doi.org/10.1016/j.renene.2021.05.131

88. Freitas PAV, González-Martínez C, Chiralt A (2023) Influence of the cellulose purification process on the properties of aerogels obtained from rice straw. Carbohydr Polym 312:120805. https://doi.org/10.1016/j.carbpol.2023.120805

89. Wang ZK, Li H, Lin XC et al (2020) Novel recyclable deep eutectic solvent boost biomass pretreatment for enzymatic hydrolysis. Bioresour Technol 307:123237. https://doi.org/10.1016/j.biortech.2020.123237

90. Shen XJ, Wen JL, Mei QQ et al (2019) Facile fractionation of lignocelluloses by biomass-derived deep eutectic solvent (DES) pretreatment for cellulose enzymatic hydrolysis and lignin valorization. Green Chem 21:275–283. https://doi.org/10.1039/c8gc03064b

91. Kim KH, Dutta T, Sun J et al (2018) Biomass pretreatment using deep eutectic solvents from lignin derived phenols. Green Chem 20:809–815. https://doi.org/10.1039/c7gc03029k

92. Wang W, Zhang C, Tong S et al (2018) Enhanced enzymatic hydrolysis and structural features of corn stover by NaOH and ozone combined pretreatment. Mol 23:1300. https://doi.org/10.3390/molecules23061300

93. Chen Z, Wang Y, Cheng H, Zhou H (2022) Hemicellulose degradation: an overlooked issue in acidic deep eutectic solvents pretreatment of lignocellulosic biomass. Ind Crops Prod 187:115335. https://doi.org/10.1016/j.indcrop.2022.115335